Multi-mode measurements in flow ducts and applications

MATS ÅBOM

KTH-THE MARCUS WALLENBERG LABORATORY

FOR SOUND AND VIBRATION RESEARCH

SE-100 44 STOCKHOLM

MATSABOM@KTH.SE

CONTENTS

BACKGROUND

BACKGROUND

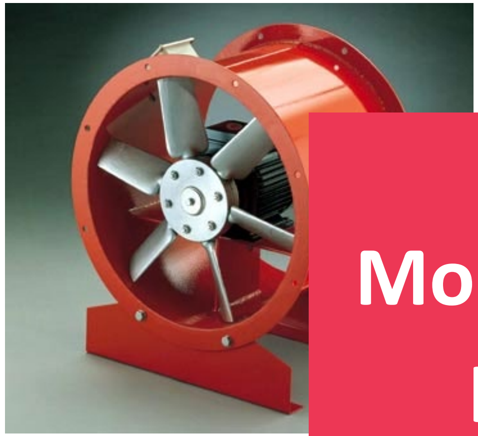

No free-field!
Most fluid- or turbomachinery problems correspond to confined flows in pipe or duct systems…

Aeroacoustics - Started around 1950´s related to noise issues with the then new jet powered civil aircrafts…

$$\frac{1}{c_0^2}\frac{\partial^2 p'}{\partial t^2}-\nabla^2 p' = s$$

Lighthills acoustic analogy

Sir Michael JAMES Lighthill FRS

(1924-1998)

Limitations in Lighthill´s theory

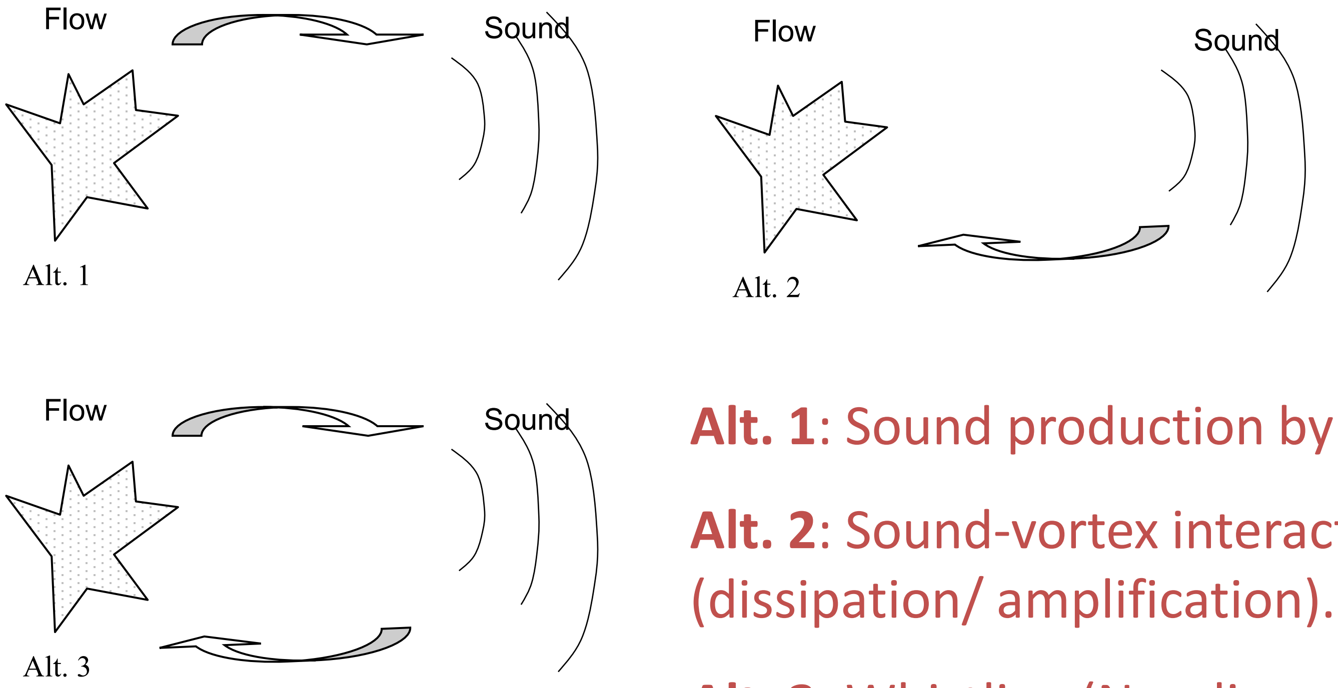

Alt. 1: Sound production by a flow.

Alt. 2: Sound-vortex interaction (dissipation/ amplification).

Alt. 3: Whistling (Non-linear Aero-Acoustics)

Limitations in Lighthill´s theory

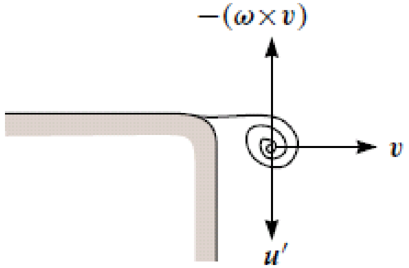

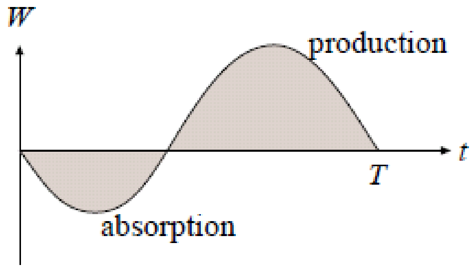

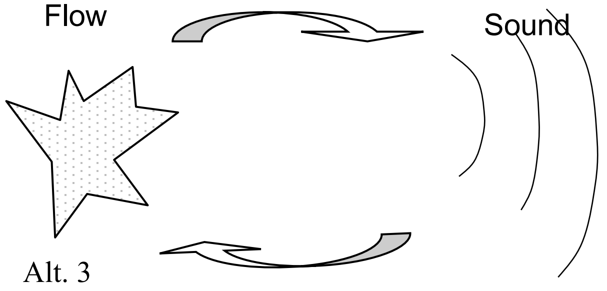

Alt. 1: Sound production by a flow.

Alt. 2: Sound-vortex interaction (dissipation/ amplification).

Alt. 3: Whistling (Non-linear Aero-Acoustics)

Limitations in Lighthill´s theory

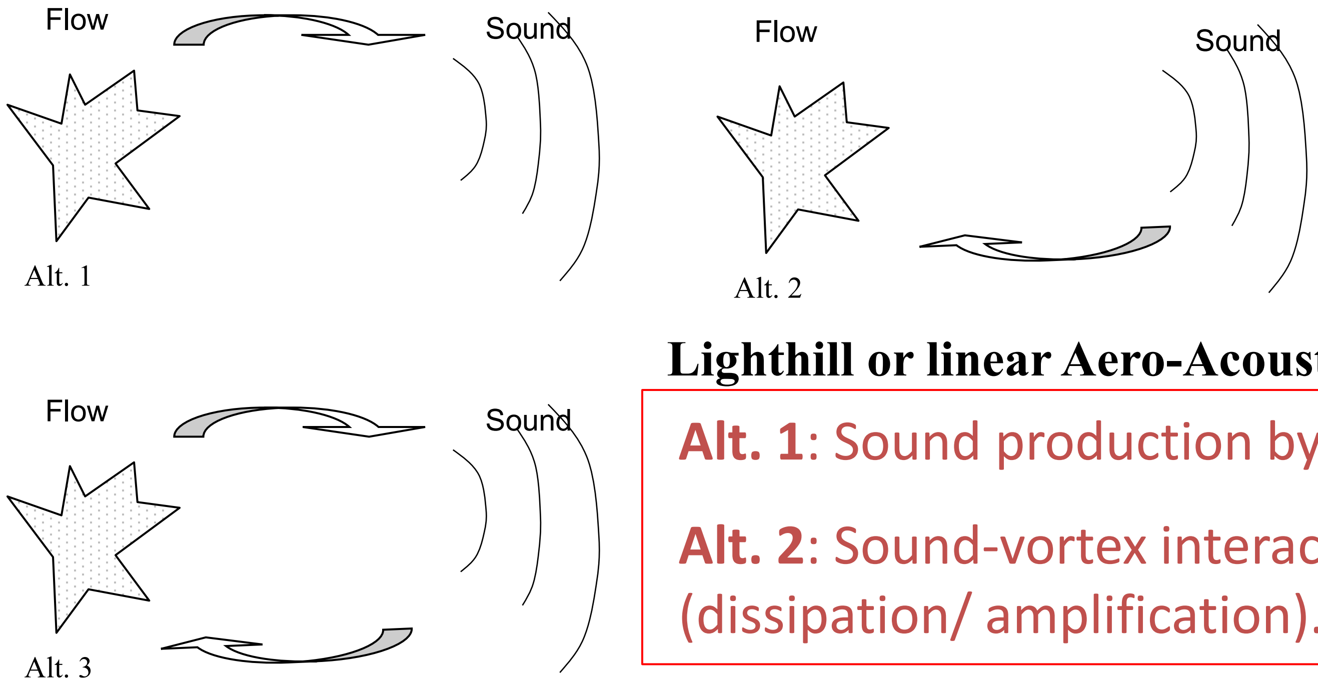

Lighthill or linear Aero-Acoustics is OK

Alt. 1: Sound production by a flow.

Alt. 2: Sound-vortex interaction (dissipation/ amplification).

Alt. 3: Whistling (Non-linear Aero-Acoustics)

ACOUSTIC INSTALLATION EFFECTS (”No free-field”)

- In the low frequency (plane wave) range ($f < f_{cut\text{-}on}$) a source is strongly coupled to a system and the acoustic output (power) can vary strongly.

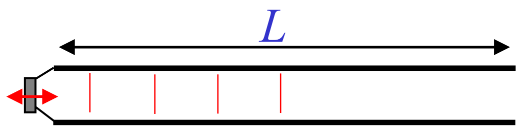

Duct excited by a loudspeaker

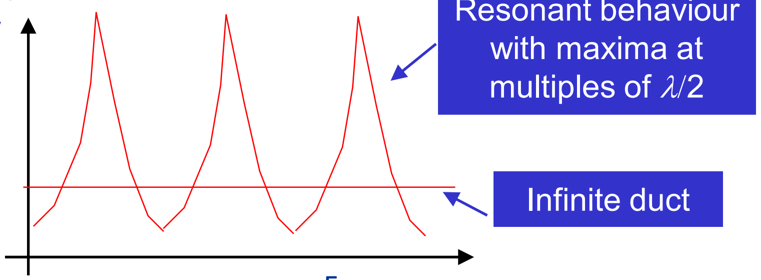

- In the mid frequency range up to (2-3)x $f_{cut\text{-}on}$, *plane + non-plane waves* exist. Also in this range strong coupling between source and system is possible.

- In the high frequency range $f >> 3xf_{cut\text{-}on}$, sound propagates as rays, there is no coupling between a source and a system and the acoustic power equals the free field value.

ACOUSTIC INSTALLATION EFFECTS ("No free-field")

- In the low frequency (plane wave) range ($f < f_{cut\text{-}on}$) a source is strongly coupled to a system and the acoustic output (power) can vary strongly.

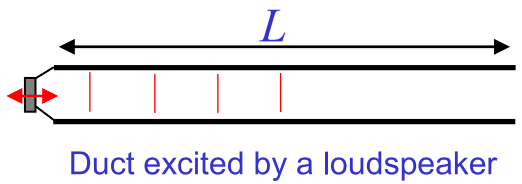

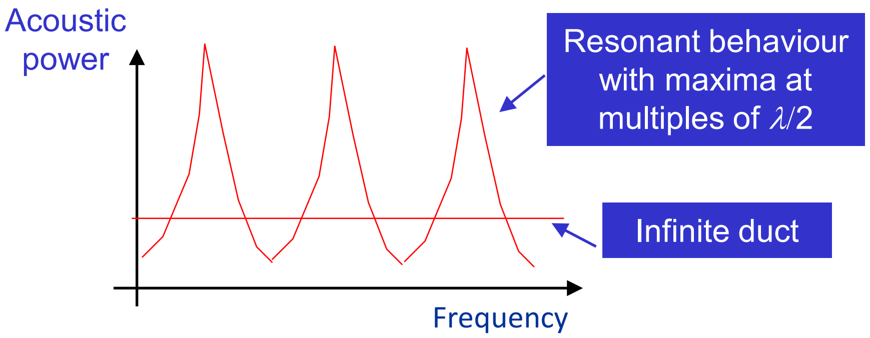

- In the mid frequency range up to (2-3)x $f_{cut\text{-}on}$, *plane + non-plane waves* exist. Also in this range strong coupling between source and system is possible.

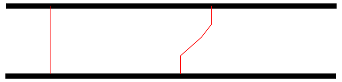

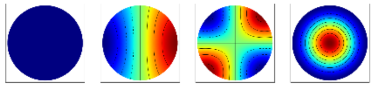

- In the high frequency range $f >> 3x f_{cut\text{-}on}$, sound propagates as rays, there is no coupling between a source and a system and the acoustic power equals the free field value.

ACOUSTIC INSTALLATION EFFECTS ("No free-field")

Coupled models required

- In the low frequency (plane wave) range ($f < f_{cut\text{-}on}$) a source is strongly coupled to a system and the acoustic output (power) can vary strongly.

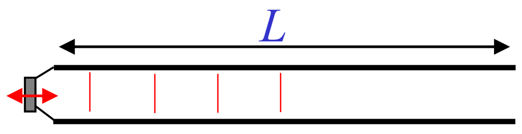

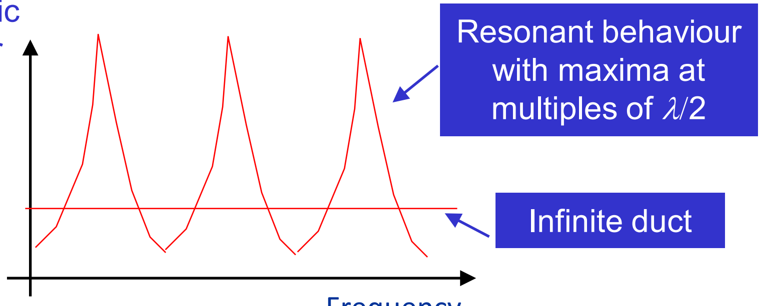

- In the mid frequency range up to (2-3)x $f_{cut\text{-}on}$, *plane + non-plane waves* exist. Also in this range strong coupling between source and system is possible.

- In the high frequency range $f >> 3xf_{cut\text{-}on}$, sound propagates as rays, there is no coupling between a source and a system and the acoustic power equals the free field value.

ACOUSTIC INSTALLATION EFFECTS (”No free-field”)

Coupled models required

- In the low frequency (plane wave) range ($f < f_{cut\text{-}on}$) a source is strongly coupled to a system and the acoustic output (power) can vary strongly.

In practice the limit is around ~ 10 propagating modes or:

$$He = kd < 3\pi,$$

where k is the wave-number and d the duct diameter.

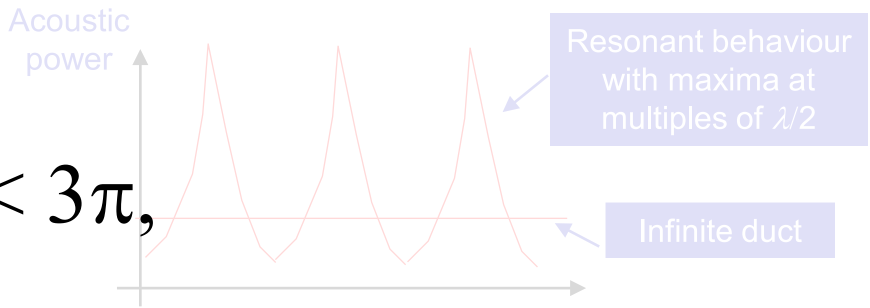

- In the mid frequency range up to (2-3)x $f_{cut\text{-}on}$, *plane + non-plane waves* exist. Also in this range strong coupling between source and system is possible.

- In the high frequency range $f >> 3xf_{cut\text{-}on}$, sound propagates as rays, there is no coupling between a source and a system and the acoustic power equals the free field value.

AEROACOUSTIC MULTI-PORTS [1-5,12]

The sound field in a duct can be expanded in propagating waves or modes:

Ψ_n:

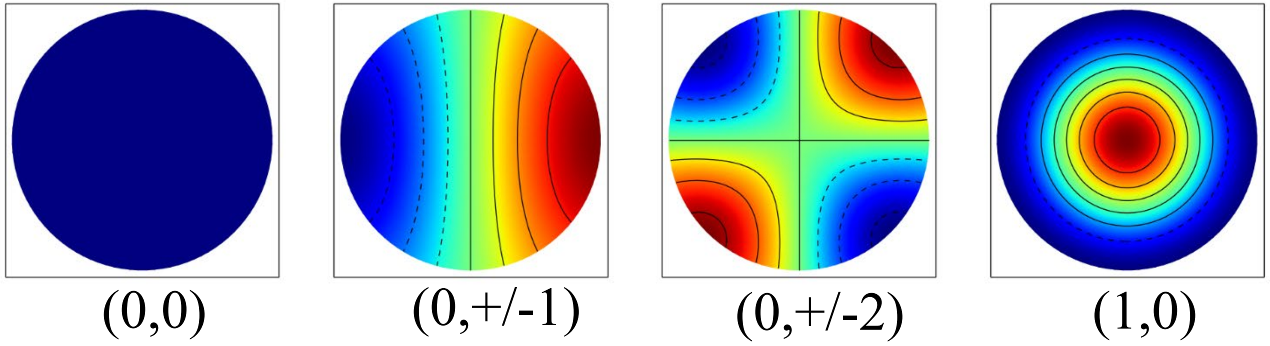

$$\hat{p}(x,y,z) = \sum_{n=0}^{N-1} \left(\hat{p}_{+n} \Psi_n(x,y) \exp(-ik_{+z,n} z) + \hat{p}_{-n} \Psi_n(x,y) \exp(ik_{-z,n} z) \right)$$

where N is at least the number of cut-on modes and z the duct axis.

AEROACOUSTIC MULTI-PORTS [1-5,12]

The sound field in a duct can be expanded in propagating waves or modes:

Ψ_n:

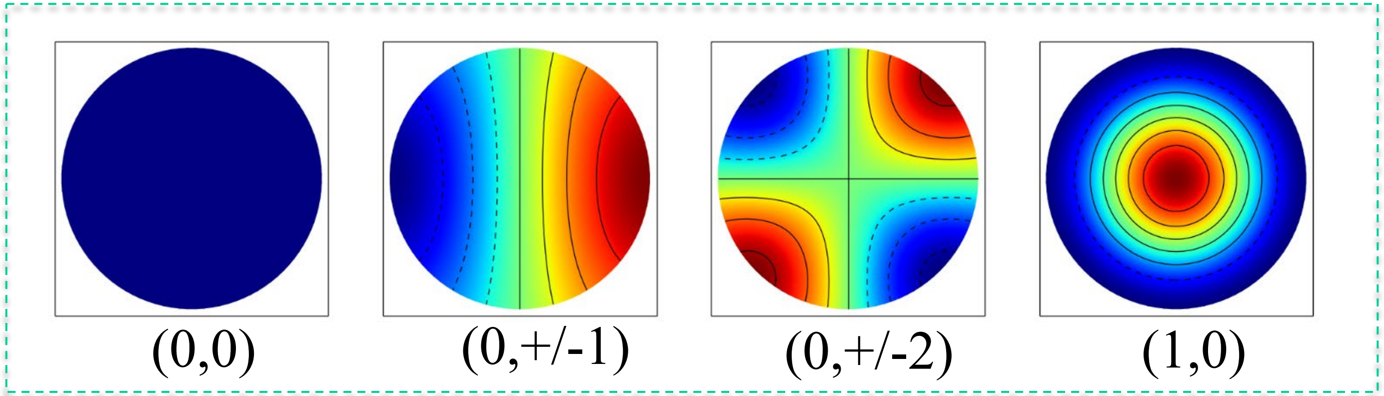

$\hat{p}($ … $)$

The eigenmodes can be based on a rigid walled duct and a plug flow forming a complete functional basis. The axial wave-number should include visco-thermal losses as described e.g. by: C Weng, F Bake (2016), Acta Acustica united Acustica 102(6), 1138-1141.

AEROACOUSTIC MULTI-PORTS [1-5,12]

The sound field in a duct can be expanded in propagating waves or modes:

Ψ_n:

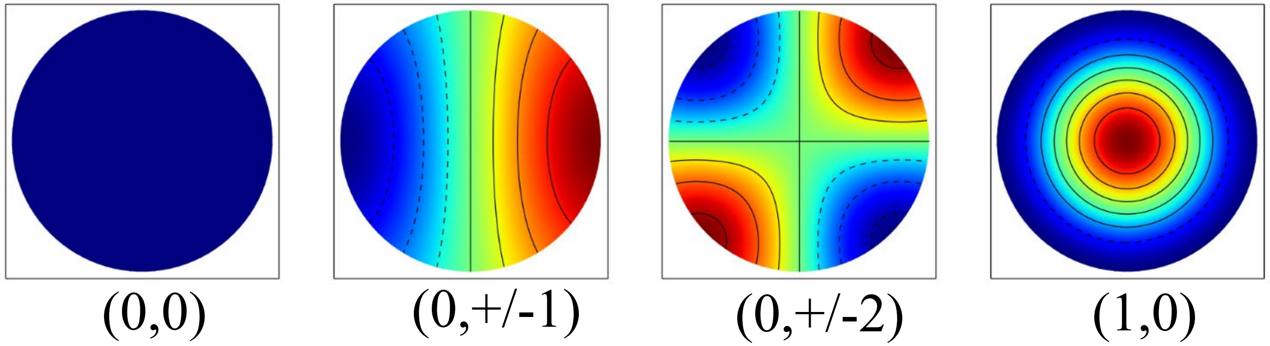

Assuming we sample the field at $M \geq 2N$ points in space we can write:

$$\left(\hat{p}_m\right) = \left[M_{mn}\right]\begin{pmatrix}\left(\hat{p}_{+n}\right)\\ \left(\hat{p}_{-n}\right)\end{pmatrix},\; M_{mn} = \Psi_n(x_m, y_m)\exp(\mp i k_{\pm z,n} z_m)$$

AEROACOUSTIC MULTI-PORTS [1-5,12]

The sound field in a duct can be expanded in propagating waves or modes:

ψ_n:

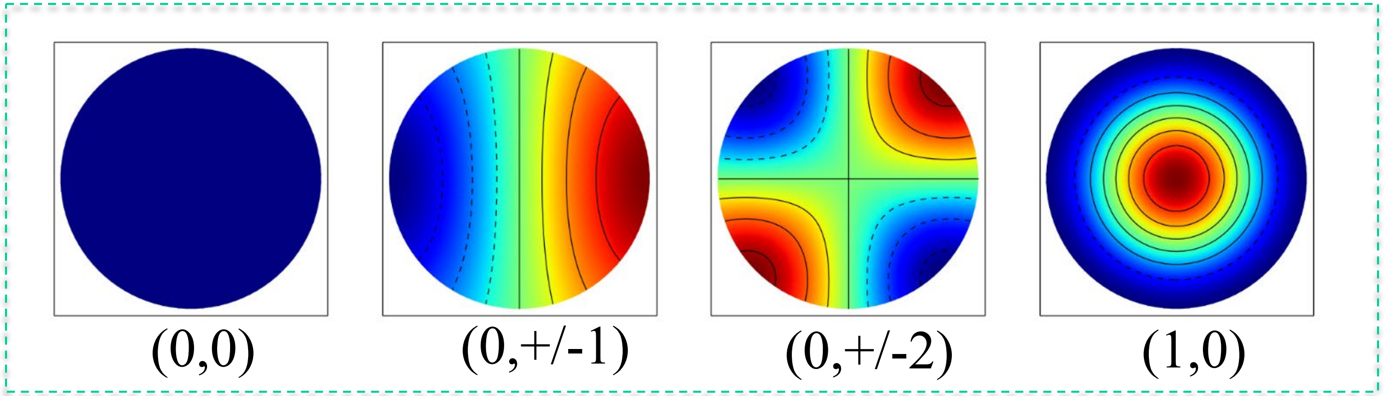

This is the basis for so called **wave decomposition methods**:

$$\mathbf{p} = \mathbf{M}\begin{pmatrix}\mathbf{p}_+\\ \mathbf{p}_-\end{pmatrix} \Rightarrow \begin{pmatrix}\mathbf{p}_+\\ \mathbf{p}_-\end{pmatrix} = \mathbf{M}^{-1}\mathbf{p}$$

The accuracy will depend on the condition number of **M**, i.e., the sampling positions.

Example: The two-microphone technique

- If only plane waves are propagating then N=1 and we get

$$\begin{pmatrix} p_1(\omega) \\ p_2(\omega) \end{pmatrix} = \begin{pmatrix} 1 & 1 \\ \exp(-jk_+ s) & \exp(jk_- s) \end{pmatrix} \begin{pmatrix} p_+(\omega) \\ p_-(\omega) \end{pmatrix}$$

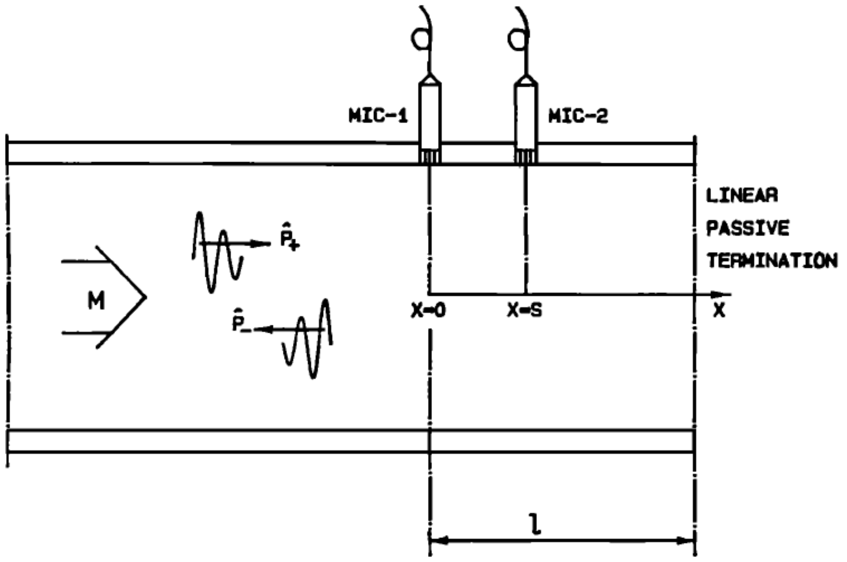

J. Y. Chung and D. A. Blaser, "Transfer function method of measuring in-duct acoustic properties. I. Theory," J. Acoust. Soc. Am. 68, 907--913

Example: Circular duct 6 modes

Condition number: $\text{cond}(\mathbf{M}) = \|\mathbf{M}\| \cdot \|\mathbf{M}^{-1}\|$

Weak singularities: $|z_2 - z_1| = l\frac{\lambda_n}{2}$ $\qquad \frac{\theta_2}{\theta_1} = \frac{\pi}{m} l \qquad l = 1,\, 2,\, 3,\, \ldots$

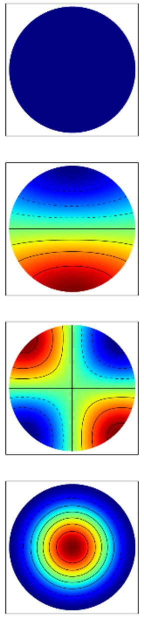

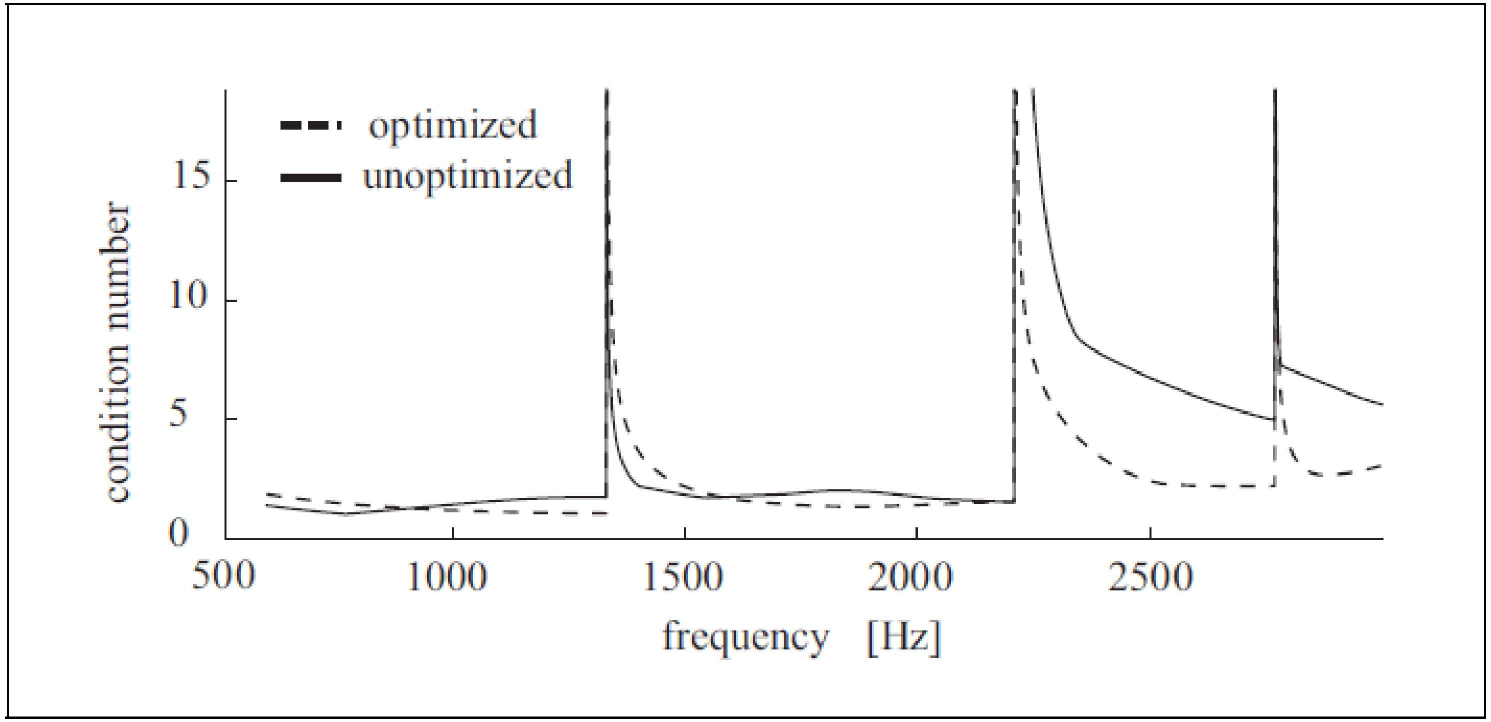

From Ref. [12] showing the effect of optimization on a configuration of 12 flush mounted microphones.

AEROACOUSTIC MULTI-PORTS [1-5,12]

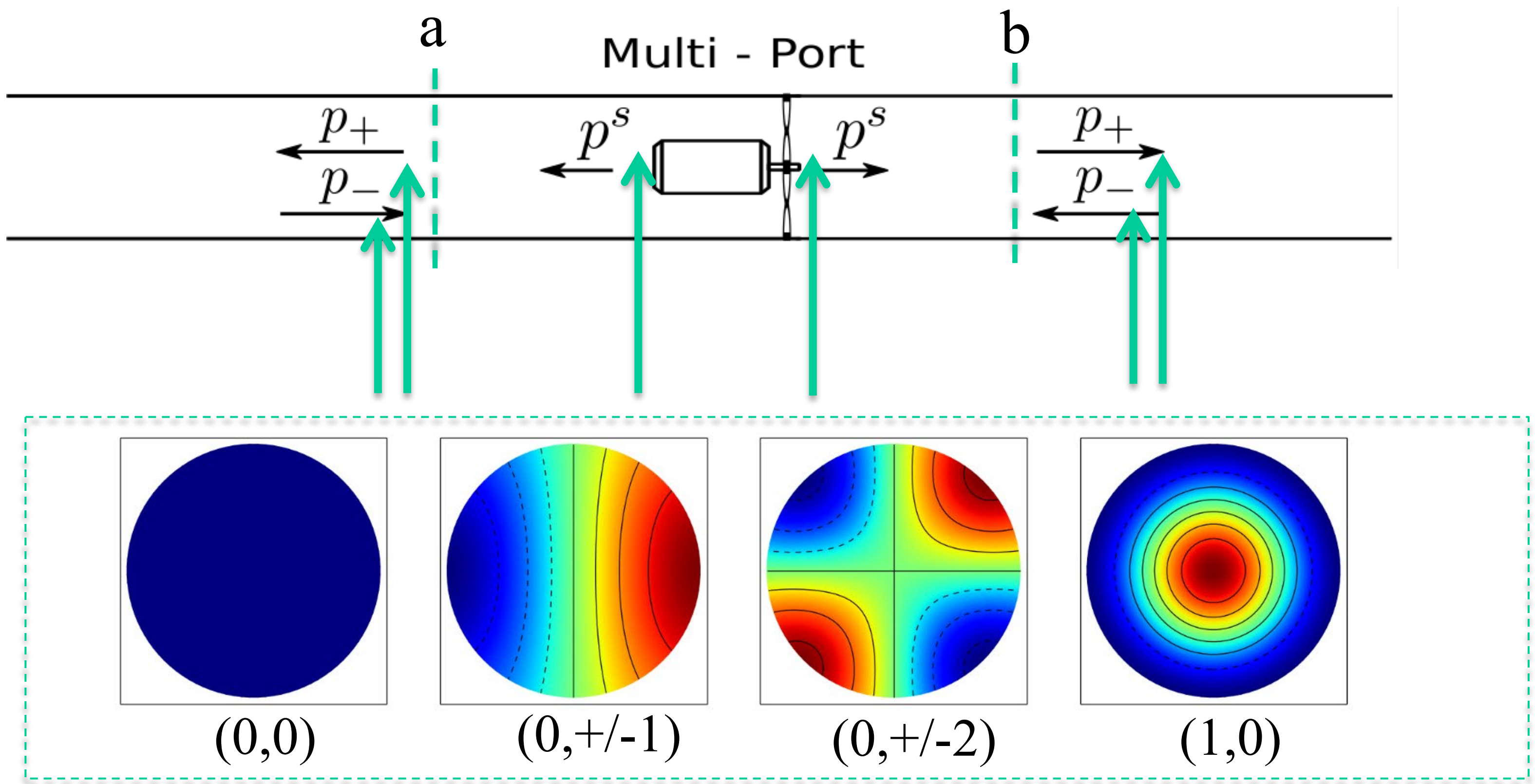

The Multi-port relates the amplitudes for modes at two (or several) **Reference cross-sections** (a&b).

AEROACOUSTIC MULTI-PORTS [1-5,12]

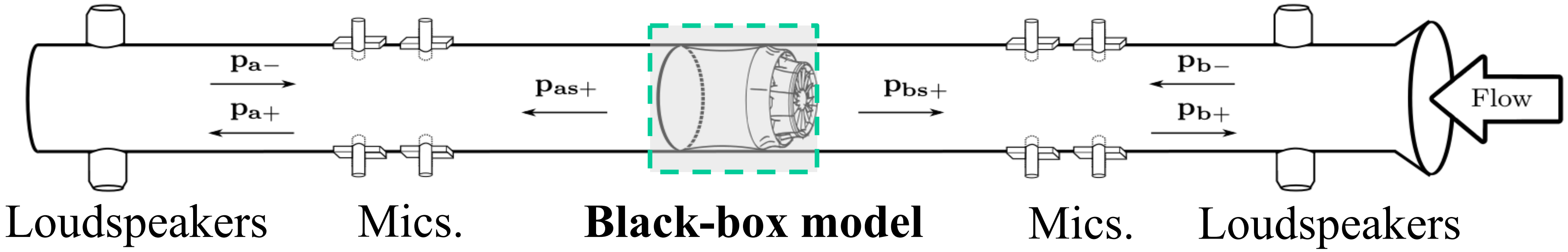

Assume **linear** and **time-invariant** systems then a multi-port in a duct can in (the Fourier domain) be characterized by

Reflection/transmission of sound

$$\underbrace{\begin{bmatrix} \mathbf{p}_{a+} \\ \mathbf{p}_{b+} \end{bmatrix}}_{\mathbf{p}_+} = \underbrace{\begin{bmatrix} \mathbf{R}_{11} & \mathbf{T}_{12} \\ \mathbf{T}_{21} & \mathbf{R}_{22} \end{bmatrix}}_{\mathbf{S}\ =\text{Passive Part}} \cdot \underbrace{\begin{bmatrix} \mathbf{p}_{a-} \\ \mathbf{p}_{b-} \end{bmatrix}}_{\mathbf{p}_-} + \underbrace{\begin{bmatrix} \mathbf{p}^s_{a+} \\ \mathbf{p}^s_{b+} \end{bmatrix}}_{\mathbf{p}^s_+ =\text{Active (Source) Part}}$$

where $\mathbf{p}_{+/-}$ represent travelling modal pressure amplitudes and **S** is the **scattering matrix** and $\mathbf{p}^s$ represents the **source part**.

AEROACOUSTIC MULTI-PORTS [1-5,12]

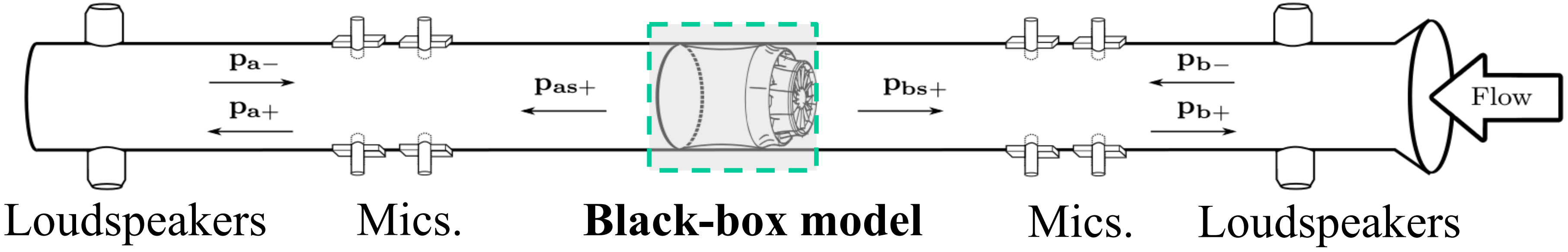

Assume linear and time-invariant systems then a multi-port in a duct can in (the Fourier domain) be characterized by

$$\underbrace{\begin{bmatrix} \mathbf{p}_{a+} \\ \mathbf{p}_{b+} \end{bmatrix}}_{\mathbf{p}_+} = \underbrace{\begin{bmatrix} \mathbf{R}_{11} & \mathbf{T}_{12} \\ \mathbf{T}_{21} & \mathbf{R}_{22} \end{bmatrix}}_{\mathbf{S}\ =\text{Passive Part}} \cdot \underbrace{\begin{bmatrix} \mathbf{p}_{a-} \\ \mathbf{p}_{b-} \end{bmatrix}}_{\mathbf{p}_-} + \underbrace{\begin{bmatrix} \mathbf{p}^s_{a+} \\ \mathbf{p}^s_{b+} \end{bmatrix}}_{\mathbf{p}^s_+\ =\text{Active (Source) Part}}$$

Reflection/transmission of sound

The classical ("first") paper suggesting this:

CREMER L. (1971) "The second annual Fairey lecture: The treatment of fans as black boxes", J. Sound Vib., 16, 1-15

AEROACOUSTIC MULTI-PORTS [1-5,12]

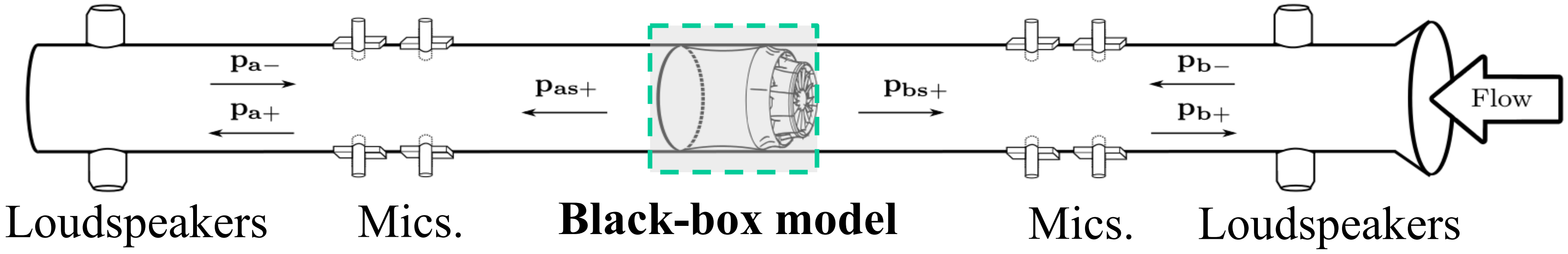

Assume linear and time-invariant systems then a multi-port in a duct can in (the Fourier domain) be characterized by

Linear Aeroacoustic model

$$\mathbf{p}_{+} = \mathbf{S}\,\mathbf{p}_{-} + \mathbf{p}_{+}^{s}$$

where $\mathbf{p}_{+/-}$ represent travelling modal pressure amplitudes and $\mathbf{S}_0$ is the **scattering matrix** and $\mathbf{p}^s$ represents the **source part**.

AEROACOUSTIC MULTI-PORTS [1-5,12]

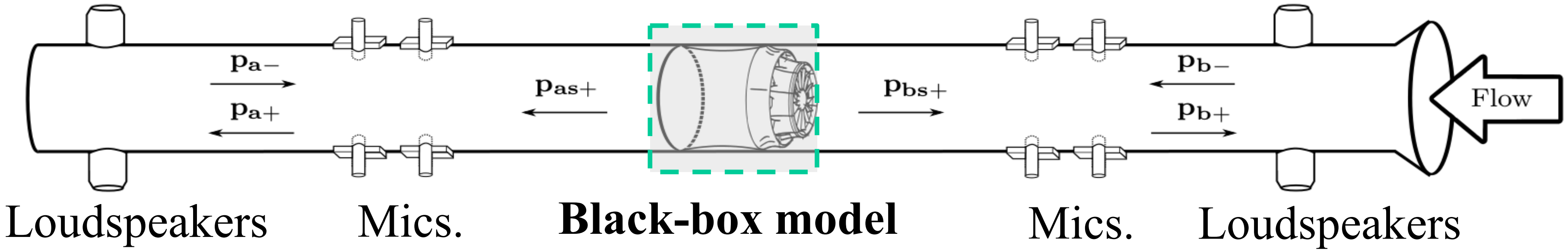

Assume linear and time-invariant systems then a multi-port in a duct can in (the Fourier domain) be characterized by

N.B. The Scattering matrix contains vortex-sound effects

$$\mathbf{p}_+ = \mathbf{S}\,\mathbf{p}_- + \mathbf{p}_+^{s}$$

Reflection-free source data

where $\mathbf{p}_{+/-}$ represent travelling modal pressure amplitudes and $\mathbf{S}_0$ is the **scattering matrix** and $\mathbf{p}^s$ represents the **source part**.

Advantages (Experimental/Numerical) of the Multi-Port Method

- Projecting the pressure field on the acoustic modes will **suppress Hydrodynamic pressure fluctuations**
- **The effects of boundary conditions are eliminated** i.e. reflection free source data can be determined
- Complex systems (low & intermediate frequency range) can be broken down into sub-elements each described by a multi-port

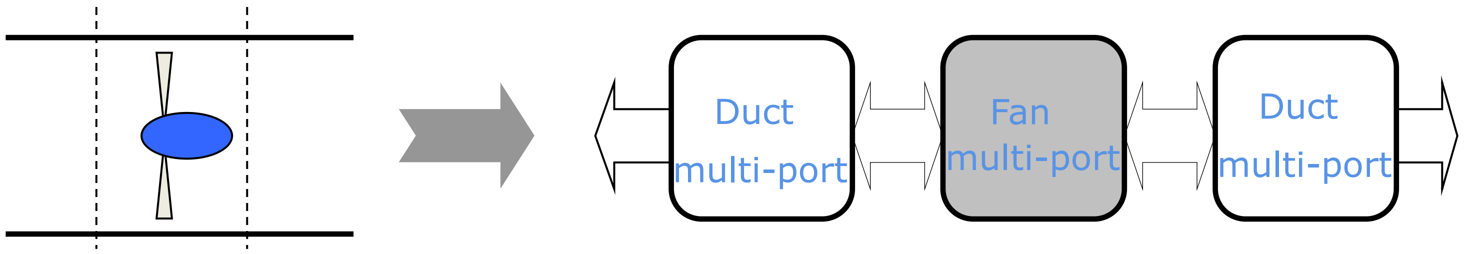

Advantages (Experimental/Numerical) of the Multi-Port Method

- Projecting the pressure field on the acoustic modes will **suppress Hydrodynamic pressure fluctuations**

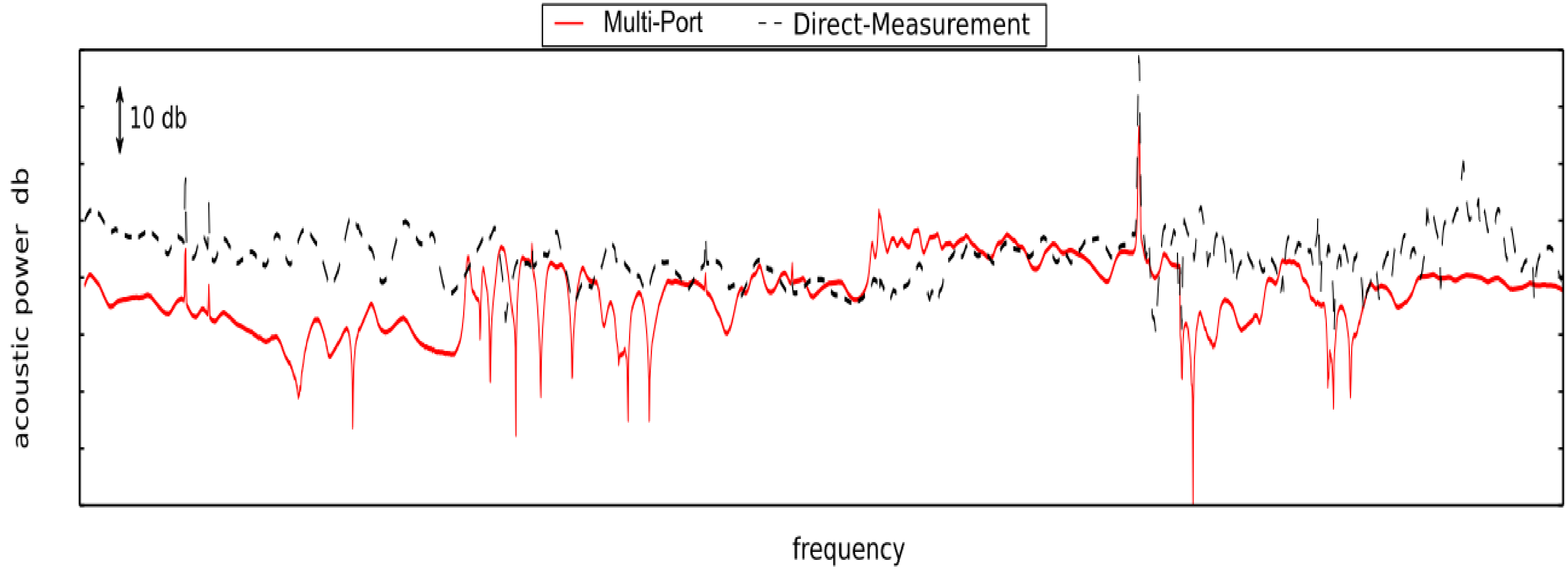

Fan measurements as part of the IdealVent project

Advantages (Experimental/Numerical) of the Multi-Port Method

- Projecting the pressure field on the acoustic modes will **suppress Hydrodynamic pressure fluctuations**
- **The effects of boundary conditions are eliminated** i.e. reflection free source data can be determined
- Complex systems (low & intermediate frequency range) can be broken down into sub-elements each described by a multi-port

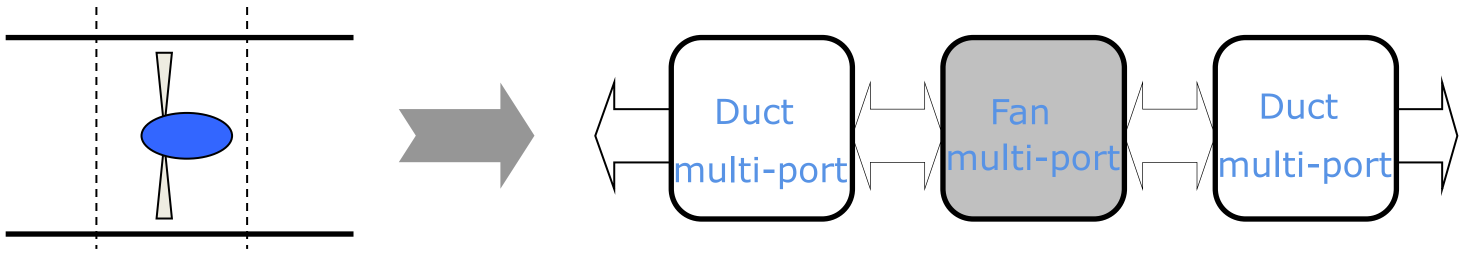

Advantages (Experimental/Numerical) of the Multi-Port Method

- Projecting the pressure field on the acoustic modes will **suppress** … **s**
- **The effect** … **ated** i.e. reflection f…
- Complex s… range) can be broken down into sub-elements each described by a multi-port

In practice the full multi-port approach is restricted to the low- and mid-frequency range or (say) 10 modes

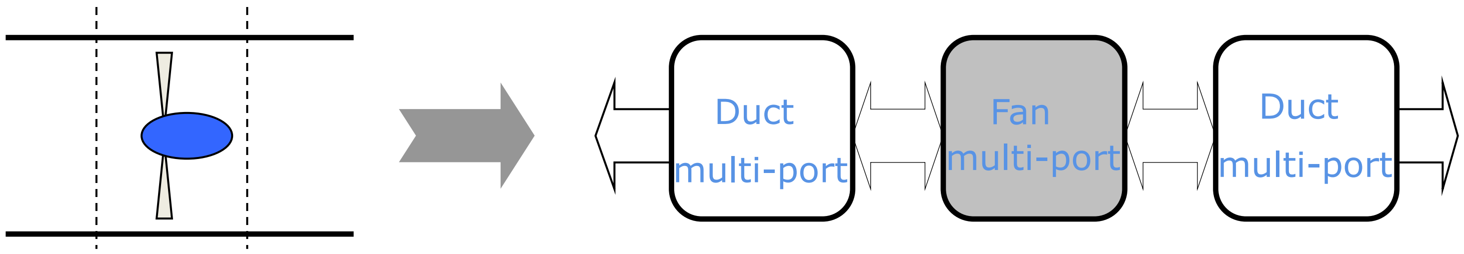

EXPERIMENTAL/NUMERICAL CHARACTERIZATION [1-15]

1) Test the multi-port using N different incident fields and measure **p+** and **p-** for each case this gives an equation for the scattering-matrix ***S***

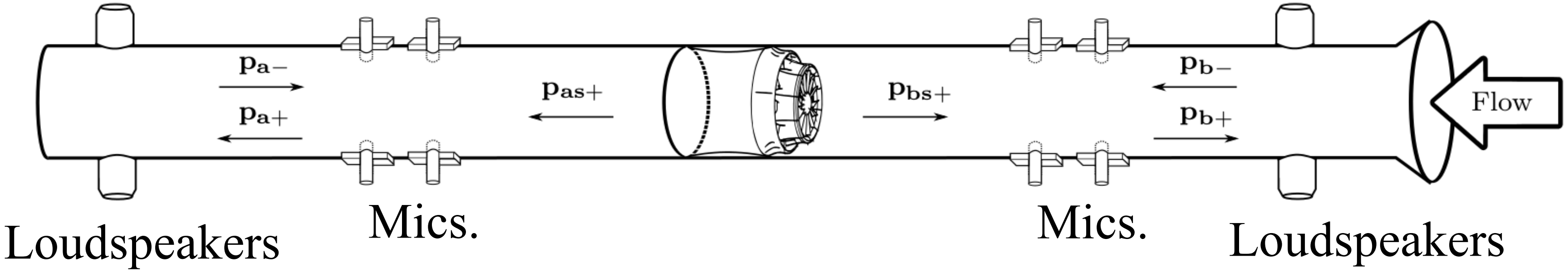

$$\mathbf{p}_+ = \mathbf{S}\,\mathbf{p}_- + \mathbf{p}_+^S$$

EXPERIMENTAL/NUMERICAL CHARACTERIZATION [1-15]

1. Test the multi-port using N different incident fields and measure **p**+ and **p**- for each case this gives an equation for the scattering-matrix $\mathbf{S}$

$$\underbrace{\left[\overbrace{\underbrace{\mathbf{p}_{0+}}_{Nx1}\ \mathbf{p}_{1+}\cdots\mathbf{p}_{(N-1)+}}^{N\ \text{vectors}}\right]}_{NxN} = \mathbf{S}\underbrace{\left[\overbrace{\underbrace{\mathbf{p}_{0-}}_{Nx1}\ \mathbf{p}_{1-}\cdots\mathbf{p}_{(N-1)-}}^{N\ \text{vectors}}\right]}_{NxN}$$

where the pressure data should be **uncorrelated** with $\mathbf{p}_+^s$ the $\mathbf{S}_0$ external source to supress

2. Once $\mathbf{p}_{s+} = \mathbf{p}_+ - \mathbf{S}\mathbf{p}_-$ is known the source strength can be directly determined from

3. This is used to estimate the source cross-spectrum matrix $\mathbf{G}_{ss} = E\left[\mathbf{p}_{s+}\mathbf{p}_{s+}^c\right]$

EXPERIMENTAL/NUMERICAL CHARACTERIZATION [1-15]

1. Test the multi-port using N different incident fields and measure **p+** and **p-** for each case this gives an equation for the scattering-matrix $\boldsymbol{S}$

$$\left[\mathbf{p}_{0+}\;\mathbf{p}_{2+}\ldots\mathbf{p}_{(N-1)+}\right]=\mathbf{S}\left[\mathbf{p}_{0-}\;\mathbf{p}_{2-}\ldots\mathbf{p}_{(N-1)-}\right]$$

where the pressure data should be correlated with the external source to supress $\mathbf{p}_{+}^{s}$

2. Once $\mathbf{S}$ is known the source strength can be directly determined from

$$\mathbf{p}_{s+}=\mathbf{p}_{+}-\mathbf{S}\mathbf{p}_{-}$$

3. This is used to estimate the source cross-spectrum matrix

$$\mathbf{G}_{ss}=E\left[\mathbf{p}_{s+}\mathbf{p}_{s+}^{c}\right]$$

EXPERIMENTAL/NUMERICAL CHARACTERIZATION [1-15]

1. Test the multi-port using N different incident fields and measure **p**+ and **p**- for each case this gives an equation for the scattering-matrix $\mathbf{S}$

$$\left[\mathbf{p}_{0+}\ \mathbf{p}_{2+}\ldots\mathbf{p}_{(N-1)+}\right]=\mathbf{S}\left[\mathbf{p}_{0-}\ \mathbf{p}_{2-}\ldots\mathbf{p}_{(N-1)-}\right]$$

where the pressure data should be correlated with the external source to supress $\mathbf{p}_{+}^{s}$

2. Once $\mathbf{S}$ is known the source strength can be directly determined from

$$\mathbf{p}_{s+}=\mathbf{p}_{+}-\mathbf{S}\mathbf{p}_{-}$$

3. This is used to estimate the source cross-spectrum matrix

$$\mathbf{G}_{ss}=E\left[\mathbf{p}_{s+}\mathbf{p}_{s+}^{c}\right]$$, c stands for the Hermitian.

EXPERIMENTAL/NUMERICAL CHARACTERIZATION [1-15]

4. For low Mach-cases the determination of the source data will suffer from bad “S/N” ratios. To improve this correlation based on sets (k) with >=2N samples in each are used

$$\mathbf{p}_{s+} = \mathbf{T}_k \mathbf{p}_{s+,k}$$

where $\mathbf{T}$ is a transfer-matrix moving the data to the reference cross-sections (a & b). [13,15]

5. For experimental determination one is limited by the number of pressure probes. A solution is then to measure the reflection matrix $\mathbf{R}$ for the test rig which leads to

$$\mathbf{p}_{s+} = (\mathbf{E}-\mathbf{SR})\mathbf{p}_{+} = \underbrace{(\mathbf{E}-\mathbf{SR})(\mathbf{E}+\mathbf{R})^{-1}}_{\mathbf{C}}\mathbf{p}$$

This formulation only requires sets with >= N data points on each side.

EXPERIMENTAL/NUMERICAL CHARACTERIZATION [1-15]

4. For low Mach-cases the determination of the source data will suffer from bad S/N ratios. To improve this correlation based on sets (k) with >=2N samples in each are used

$$\mathbf{p}_{s+} = \mathbf{T}_k \mathbf{p}_{s+,k}$$

where $\mathbf{T}$ is a transfer-matrix moving the data to the reference cross-sections (a & b). [13,15]

5. For experimental determination one is limited by the number of pressure probes. A solution is then to measure the reflection matrix $\mathbf{R}$ for the test rig which leads to

$$\mathbf{p}_{s+} = (\mathbf{E} - \mathbf{S}\mathbf{R})\mathbf{p}_{+} = \underbrace{(\mathbf{E} - \mathbf{S}\mathbf{R})(\mathbf{E} + \mathbf{R})^{-1}}_{\mathbf{C}} \mathbf{p}$$

This formulation only requires sets with >= N data points on each side compared to >= 2N for alt. 4. [2,3,5,14]

COMPARISON EXPERIMENTAL versus NUMERICAL CHARACTERIZATION

1. In **experiments** only **pressure data at the walls** are normally possible to measure.

2. In **simulations all points** can be used AND also **all fields** are known. This means wave decomposition can be based on pressure and e.g. axial velocity.

3. In **experiments** only **wall mounted sources** are normally used to determine the scattering, which makes excitation of single modes difficult. In **simulations** excitation of **single incident modes** is no problem.

4. In experiments a **low S/N** in source strength data can be handled by using a **long measurement time**. For **simulations** normally only a **short time record** is possible (~1 s). **BUT a very large number of sampling points are available**.

Examples of numerical MULTI-PORT WORKS at KTH

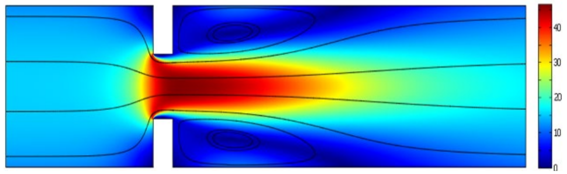

Single Orifice – **i)** Linearized Navier Stokes Equations (LNSE) – 2-port Scattering matrix & Whistling analysis;
ii) LES – Complete 2-port. [8-10]

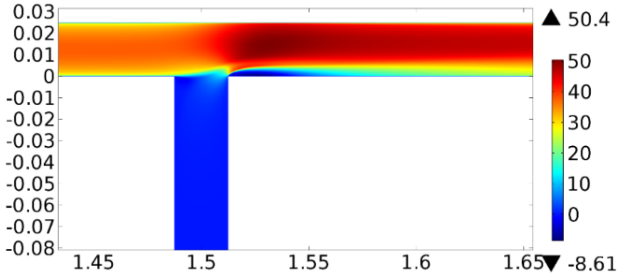

T-junction – LNSE model 3-port Scattering matrix- Sound amplification. [11]

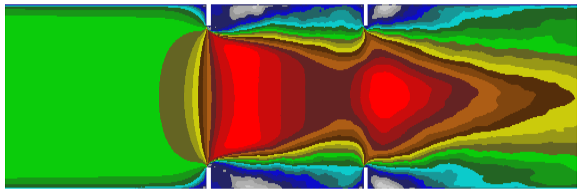

Tandem orifice configuration – Complete multi-port up to the radial mode (=6 modes); *Hybrid model* –
Scattering using LNSE, Sound generation using hybrid RANS&LES (IDDES). [14,15]

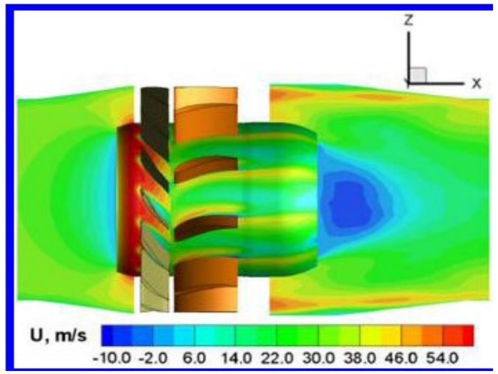

Axial compressor – Modal Source spectra using IDDES. [13]

APPLICATION EXAMPLES-Experiments

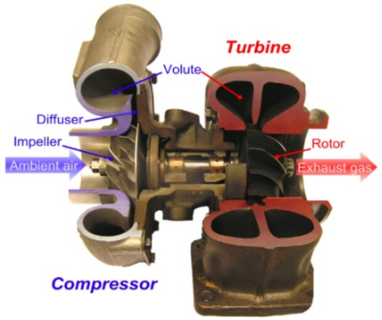

- Automotive turbo-charger [6,7]

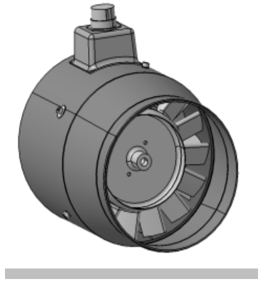

- Axial fan (IDEALVENT) [13]

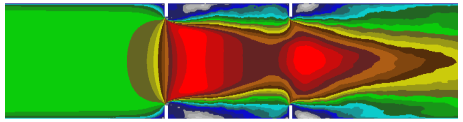

- Tandem orifice (IDEALVENT) [14,15]

Competence **C**enter for **G**as **Ex**change (CCGEx) www.ccgex.kth.se

ROYAL INSTITUTE OF TECHNOLOGY

CCGEx

- Research focus on the gas management of IC engines.
- Combined effort between KTH, the Swedish Energy Agency and some leading OEMs.
- Main research fields are fluid mechanics and acoustics.

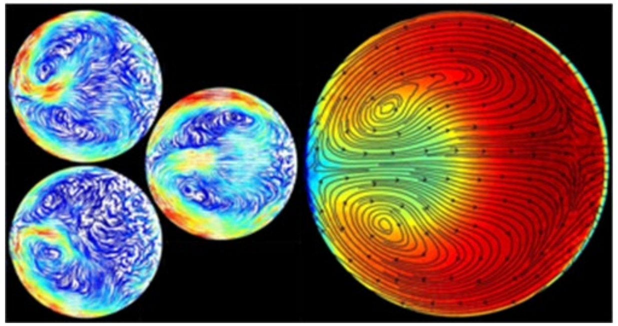

Energimyndigheten SCANIA VOLVO VOLVO BorgWarner

KTH-CCGEx Acoustic Testrig [6,7]

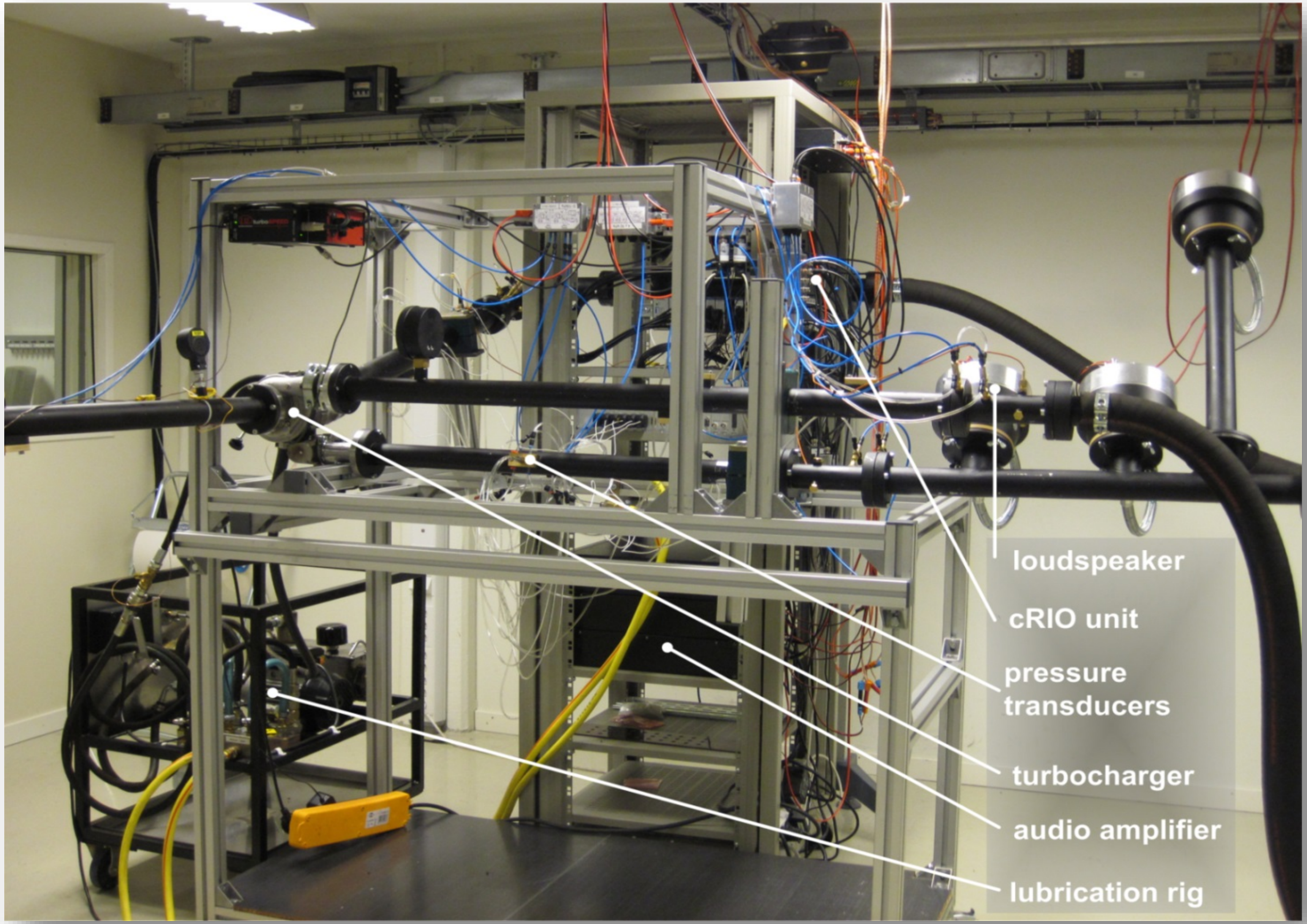

Compressor used in experiments

- Passenger car turbo-charger Garrett GT1752 driven by the compressed air feed to the turbine.
- Inlet diam. is 44mm.
- Outlet diam. is 42mm.
- The rotor has 6 (+6 splitter) blades.
- Shaft frequency ~80…180kRPM – blade pass frequency 8…18kHz.

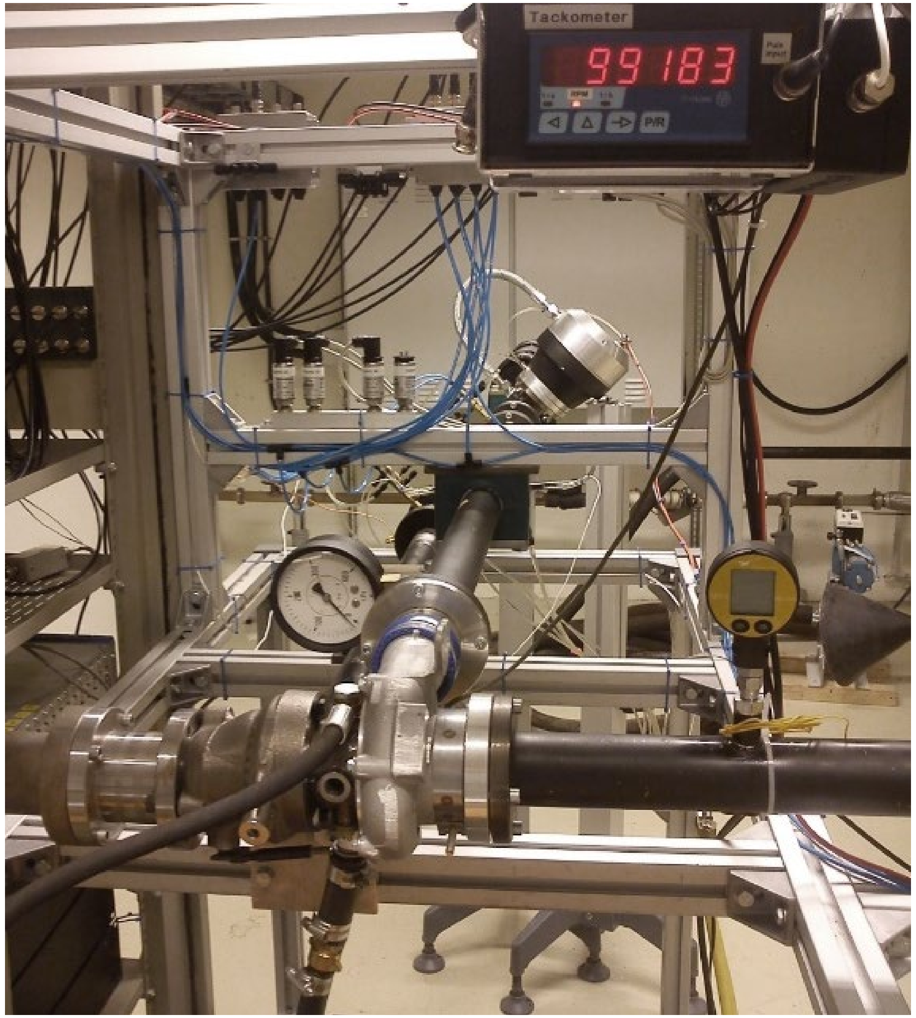

Acoustic 2-port formulation

$$f_c = \frac{1.814 \cdot c}{\pi d}$$

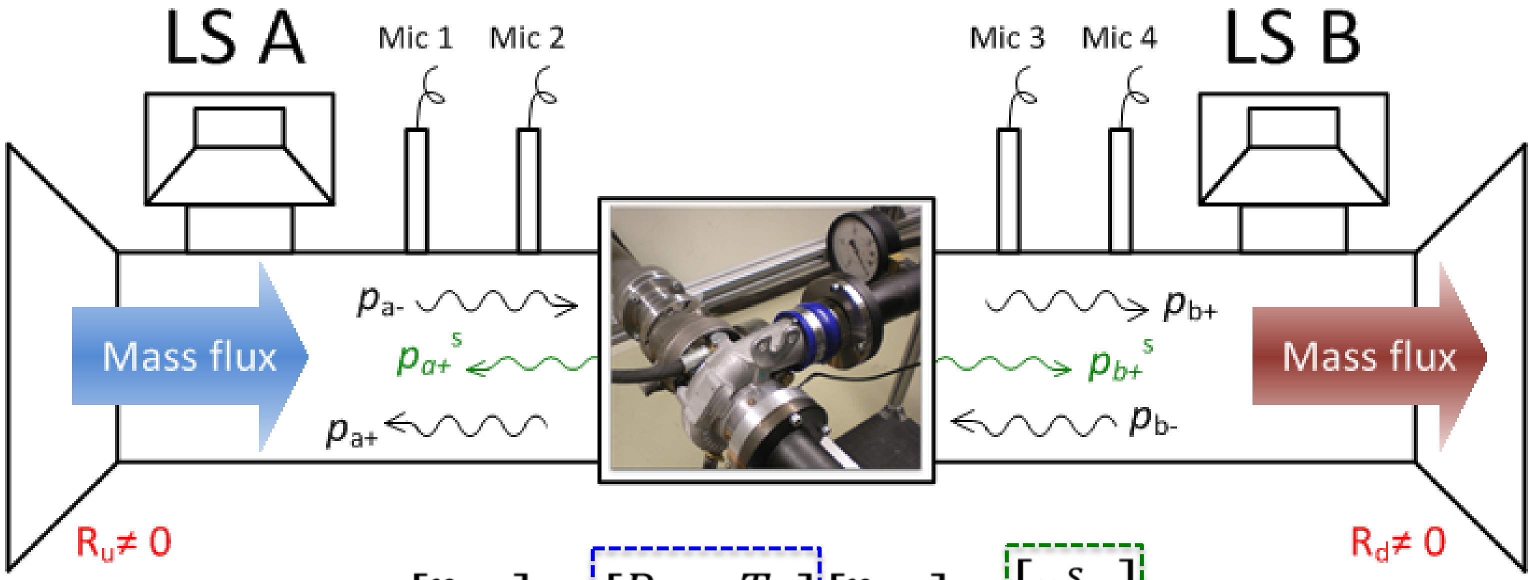

$$\begin{bmatrix} p_{a+} \\ p_{b+} \end{bmatrix} = \begin{bmatrix} R_a & T_b \\ T_a & R_b \end{bmatrix} \begin{bmatrix} p_{a-} \\ p_{b-} \end{bmatrix} + \begin{bmatrix} p_{a+}^{s} \\ p_{b+}^{s} \end{bmatrix}$$

S-matrix

- The acoustical performance of a flow duct element is determined by the full 2-port model which consists both the passive and the active parts.

Reflection-free sound generation

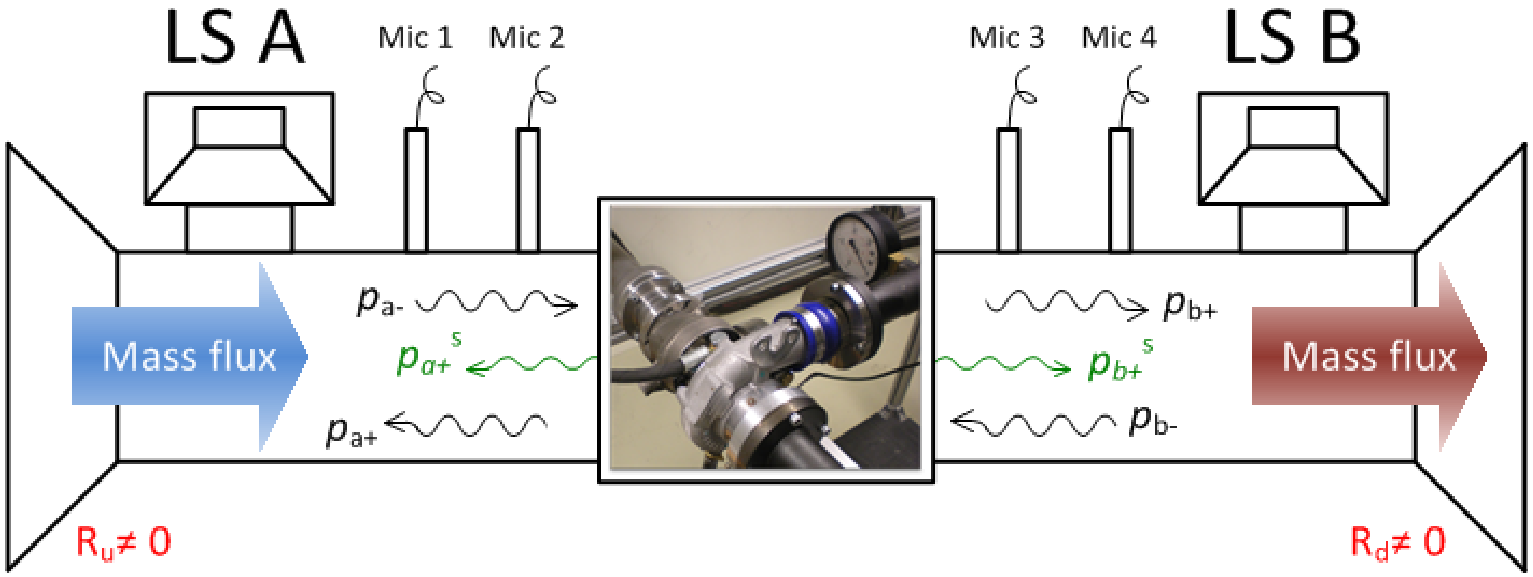

$$\boldsymbol{p}_+^s = (\boldsymbol{E} - \boldsymbol{SR})(\boldsymbol{E} + \boldsymbol{R})^{-1}\boldsymbol{p}$$

$$\boldsymbol{G}^s = \boldsymbol{p}_s(\boldsymbol{p}_s')^{\dagger} = \begin{bmatrix} G_{p_a^s p_a^s} & G_{p_b^s p_a^s} \\ G_{p_a^s p_b^s} & G_{p_b^s p_b^s} \end{bmatrix}$$

Sound generation of the compressor [7]

- The following can be observed while operating close to deep surge:
  - a large (up to 25dB) broadband increase of SPL;
  - an additional generation of sound at ~.5 of shaft rotating order.

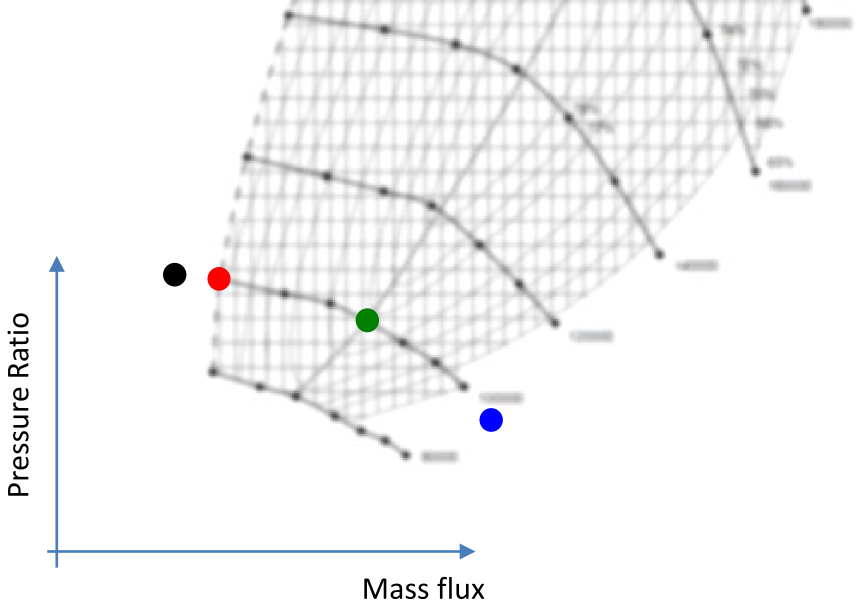

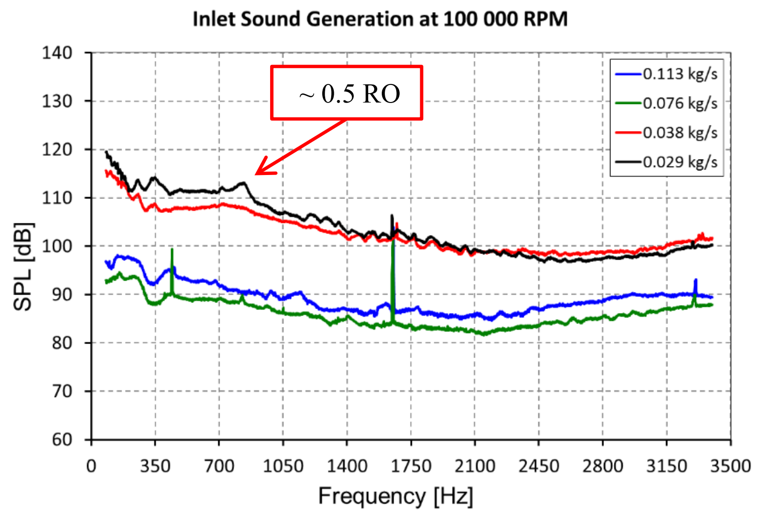

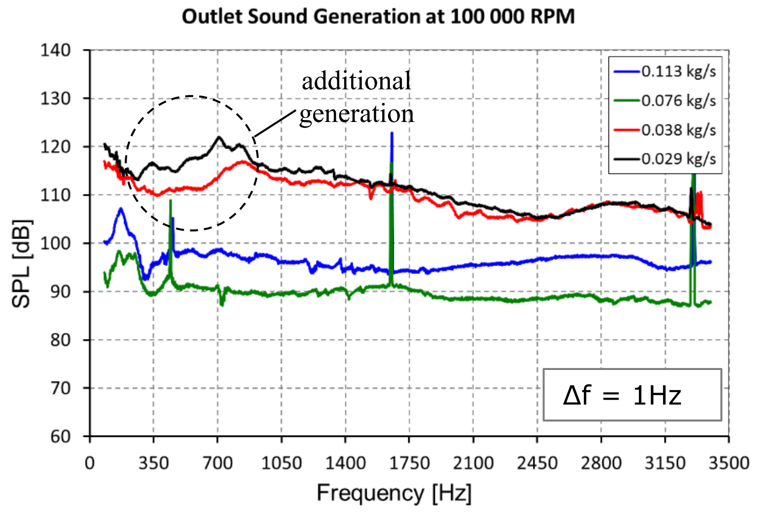

Aero-acoustic coupling [7]

- From the S-matrix **dissipation (-) or amplification (+)** of the compressor can be computed.
- The data shows that approaching surge amplifying flow instabilities, e.g., at ~0.5 RO occur. But the overall losses still dominate.
- **The only possibility for a self sustained oscillation ("strong surge") is below 100 Hz**.

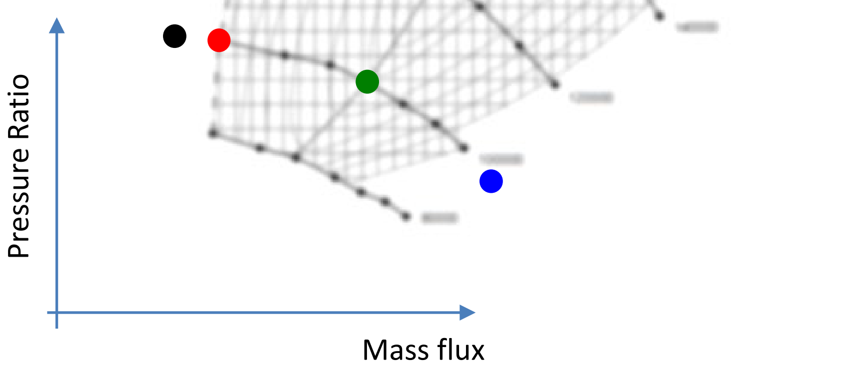

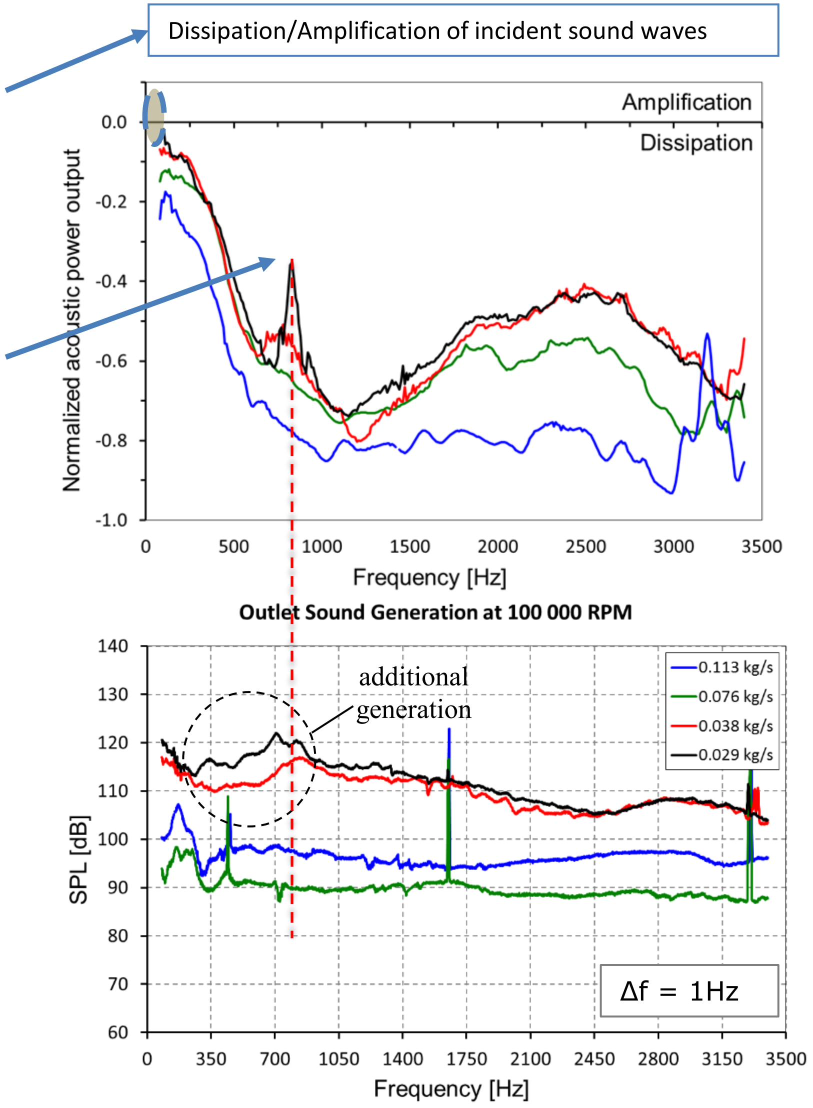

AIRCRAFT CLIMATE CONTROL SYSTEMS

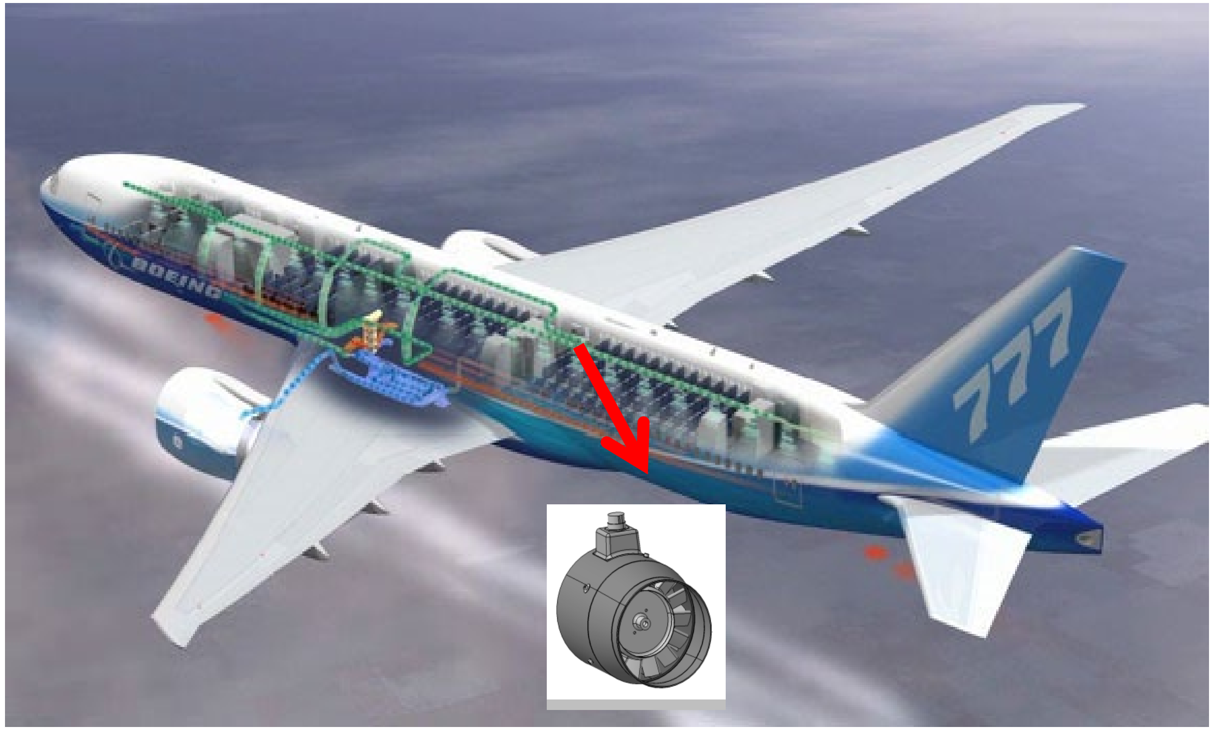

Overview of results (exp&num) in the project involving KTH

- Analysis (IDDES=RANS+LES) of an axial Liebherr fan unit for aircraft climate systems [13]
- Analysis of single and double diaphragms (orifices) [14,15]
- Novel noise control concepts involving Micro-Perforated-Plates (MPP:s)

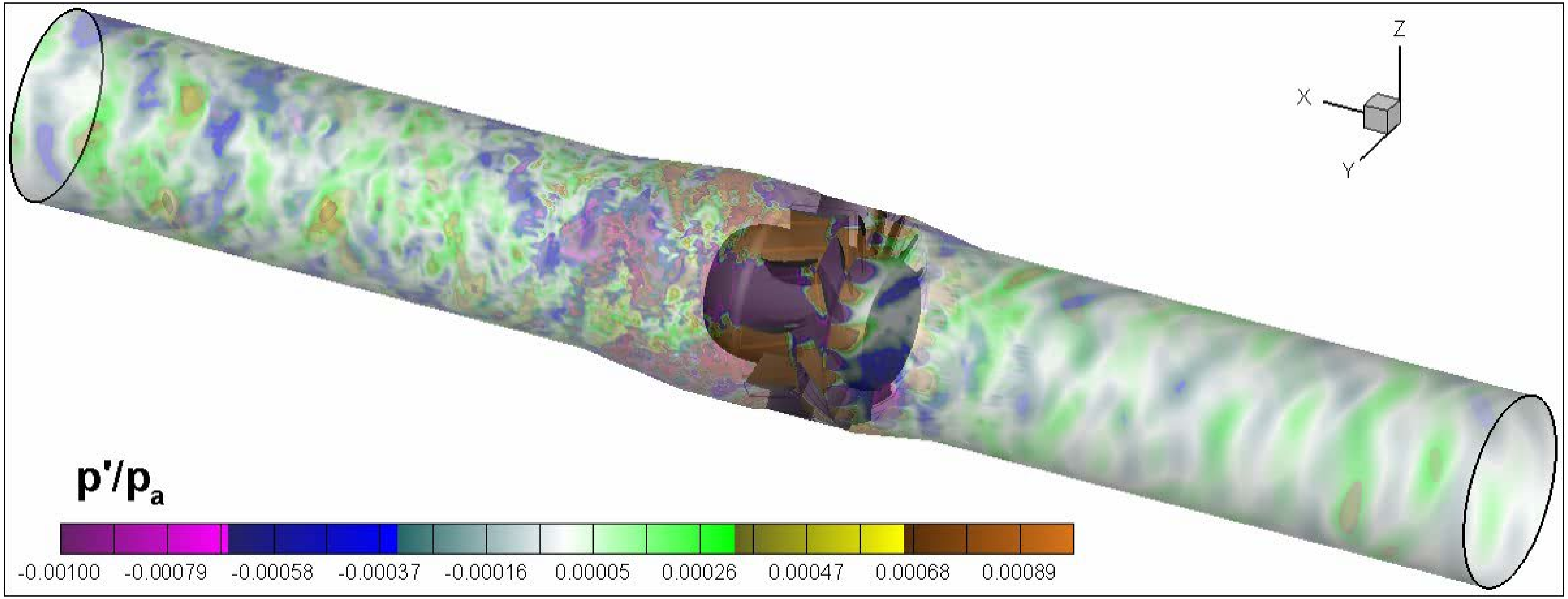

Installation effects are an important aspect of the project

Note there are two types: **Acoustic** and **Aerodynamic**.

- The Acoustic means the the acoustic nearfields (= non-cut on modes) must have decayed at the next element.
- The Aerodynamic means that the inflow to the next element should be back to a “normal” straight pipe condition, i.e., the flow near-fields should have decayed.

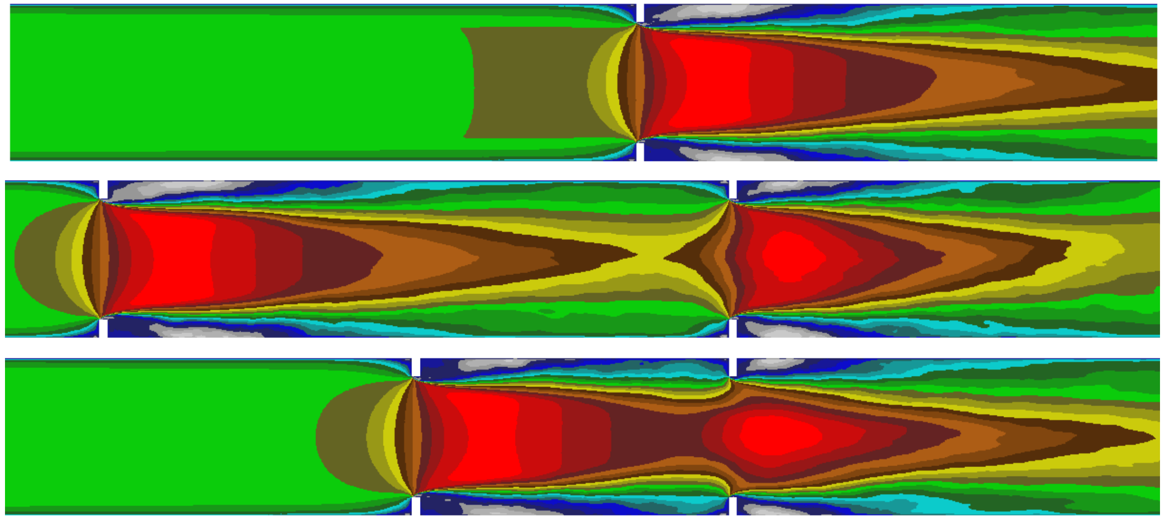

Test rig built by VKI & KTH

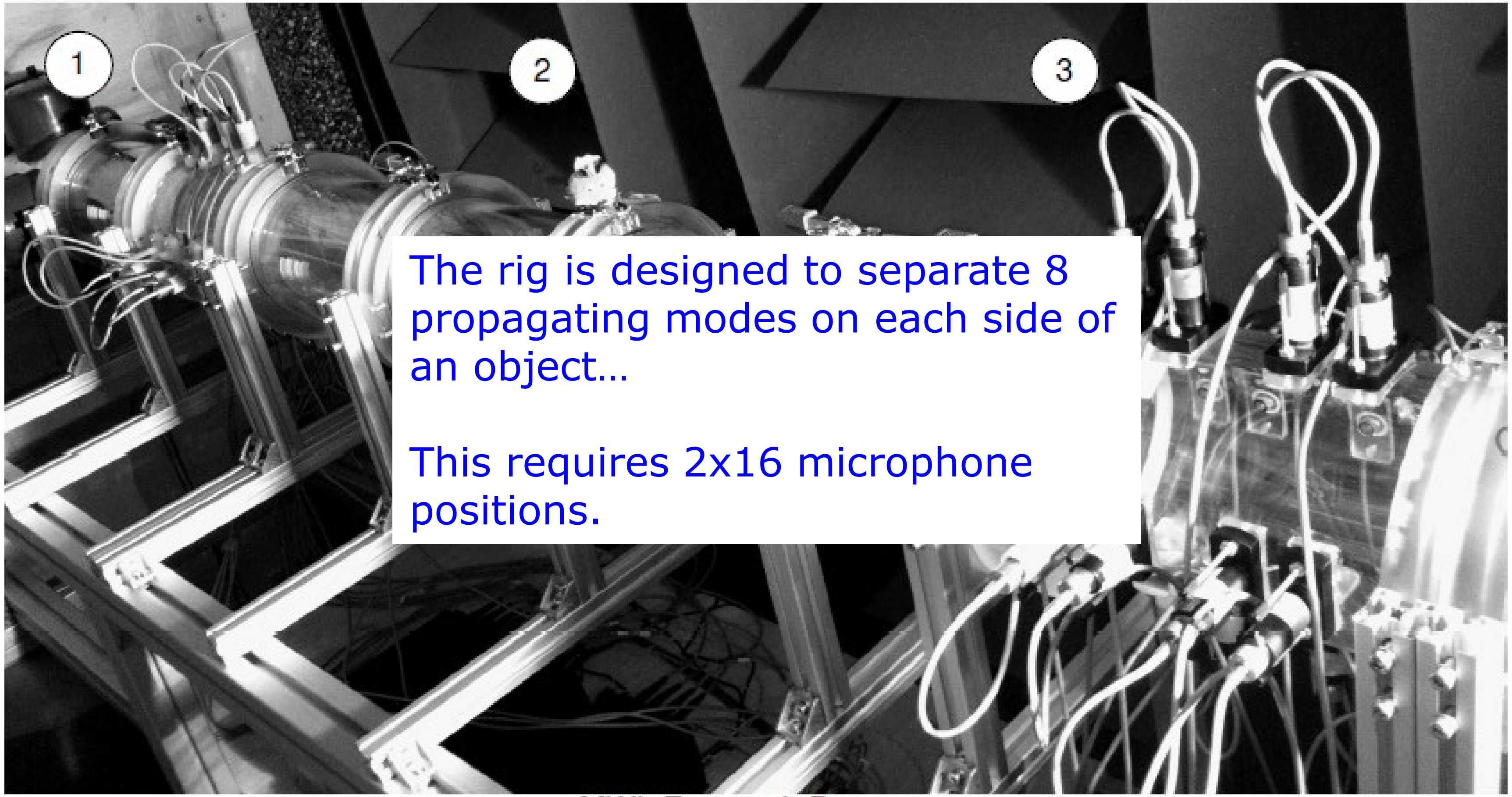

The rig is designed to separate 8 propagating modes on each side of an object…

This requires 2x16 microphone positions.

Axial compressor spectrum [13]

- Axial compressor with strong BPF (2700 Hz) and higher order mode conten

- The (0,0) & (2,0)
- modes are
- particularly strong

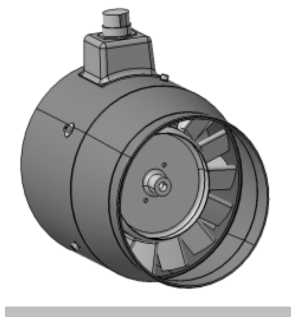

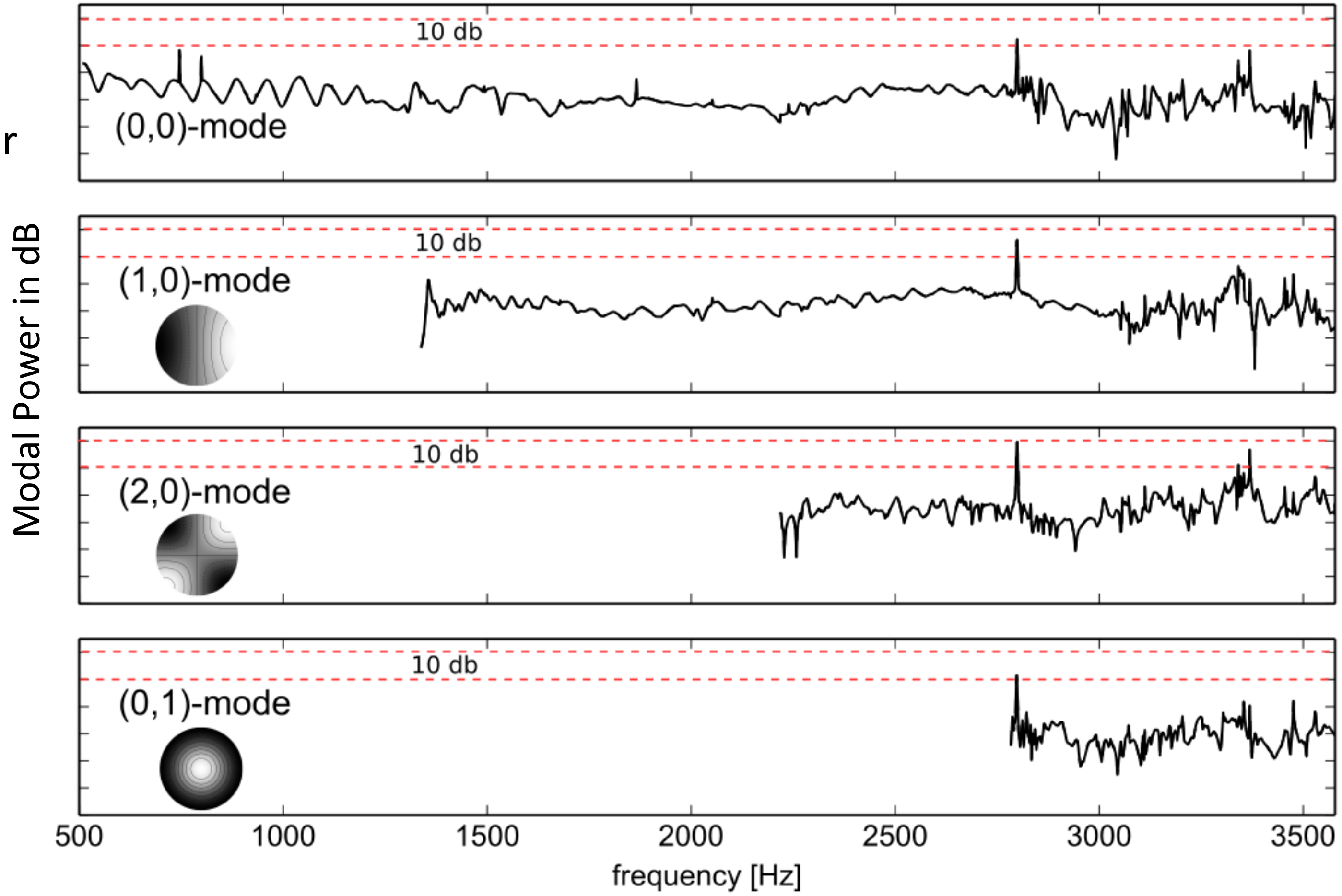

Installation effects – Single&Tandem Orifices [14,15]

Orifice-plate in a circular duct

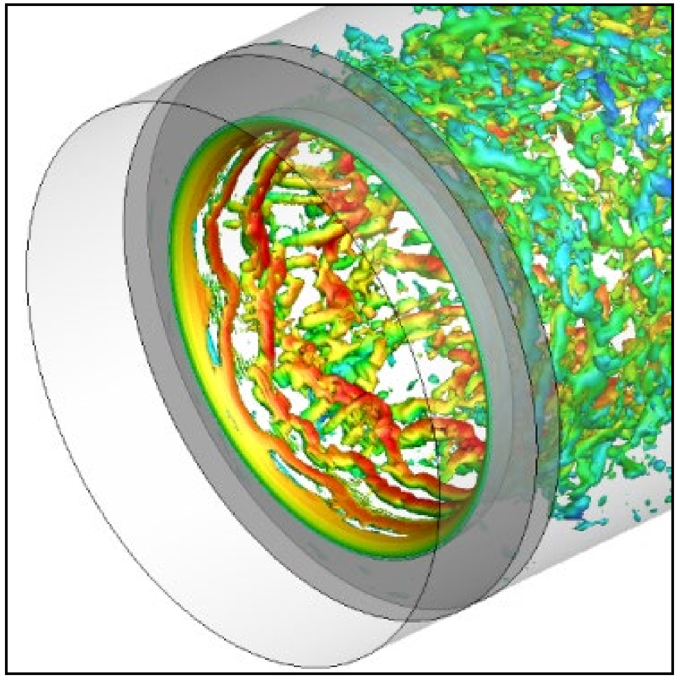

Active part computed by IDDES and **the passive** by Linearized Navier Stokes Eqs. (LNSE).

BUT here we will only present the experimental part.

Objectives

Investigating the **effect of installation (acoustic & aerodynamic)** on the **acoustic properties** of induct orifice plates (separation 2D, 4D and 10D)

The problem is simplified to a **single (<u>clean</u>) orifice** and a **tandem – orifice** configuration

Orifice u-velocity, m/s 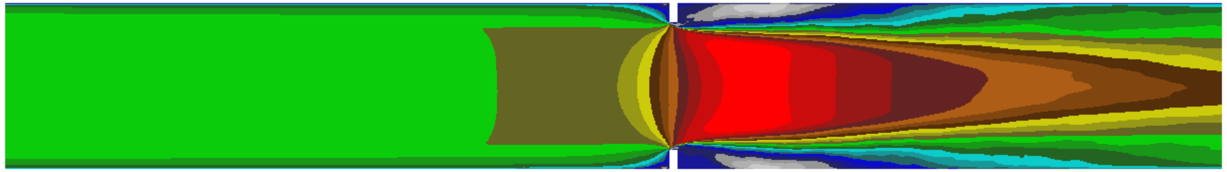	**Single**
Orifice ocity, m/s 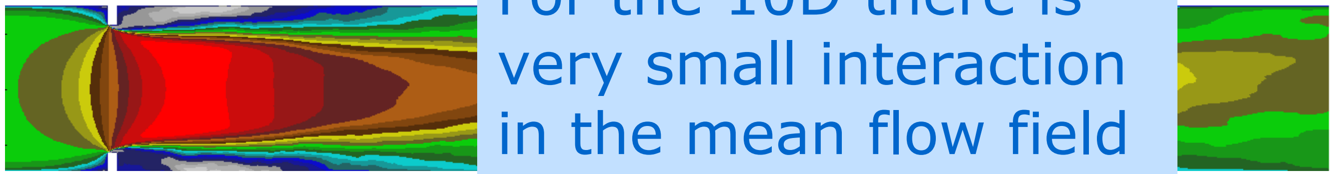 For the 10D there is very small interaction in the mean flow field	**Tandem sep. 4D**
Orifice Orifice u-velocity, m/s 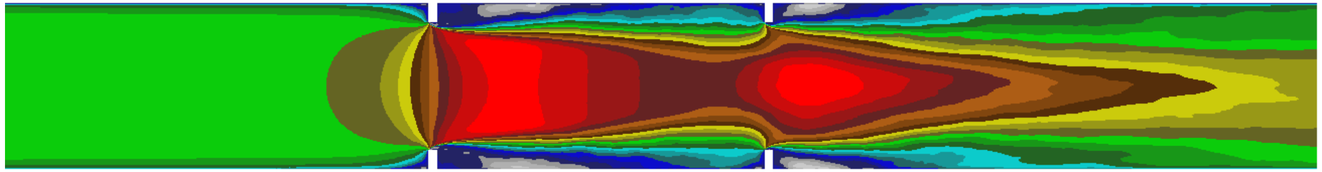	**Tandem sep. 2D**

Objectives

The problem is split into sub problems

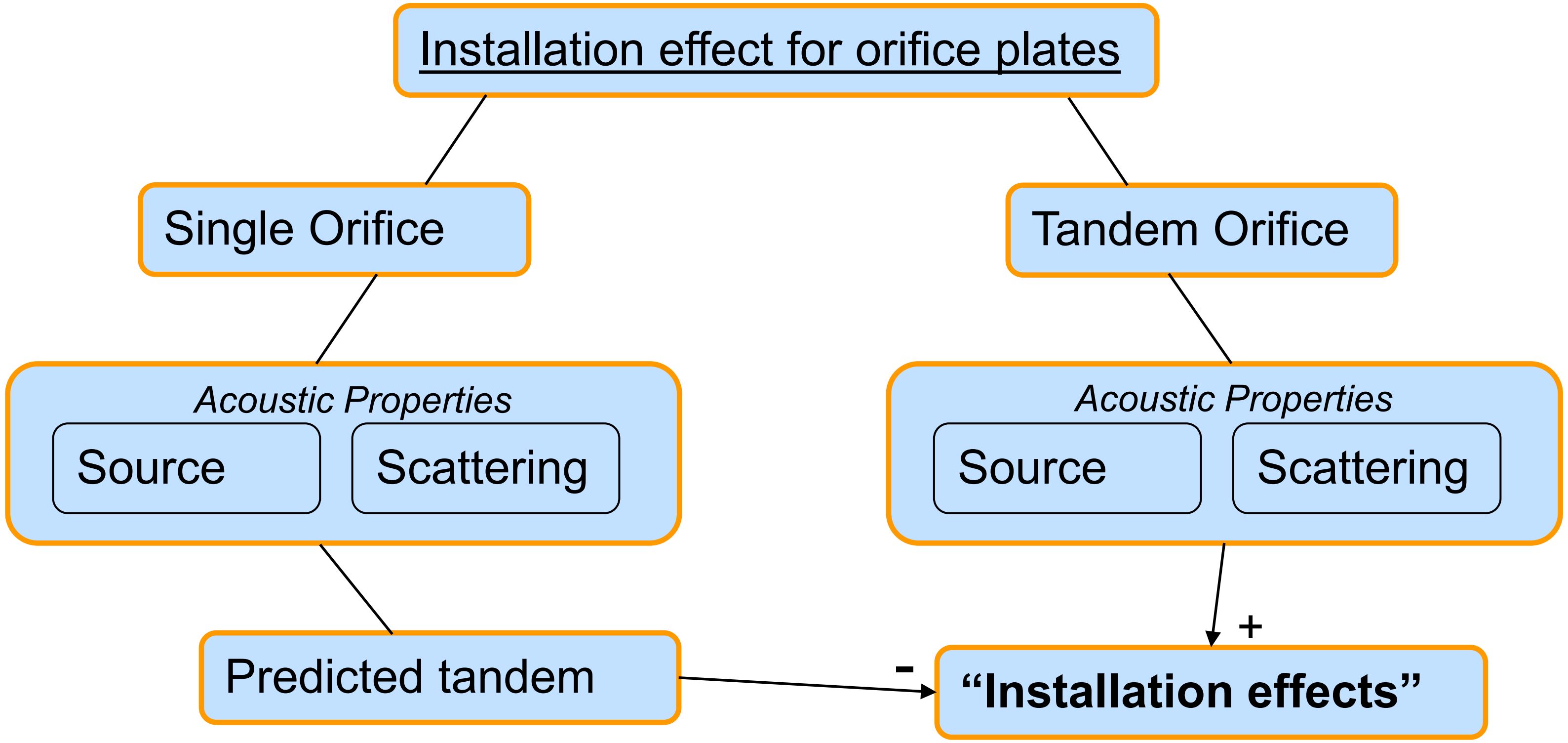

The **installation effects** will simply be **the difference** between 'predicted' and 'real'.

The **Scattering Matrices** will "handle" the acoustic installation effects **BUT** the multi-port **Source strength** assumes an undisturbed inflow….

Orifice Measurements

Measurements for model-validation at the Marcus Wallenberg Laboratory for Sound and Vibration Research at KTH

Measurements for model-validation at the *Marcus Wallenberg Laboratory for Sound and Vibration Research at KTH*

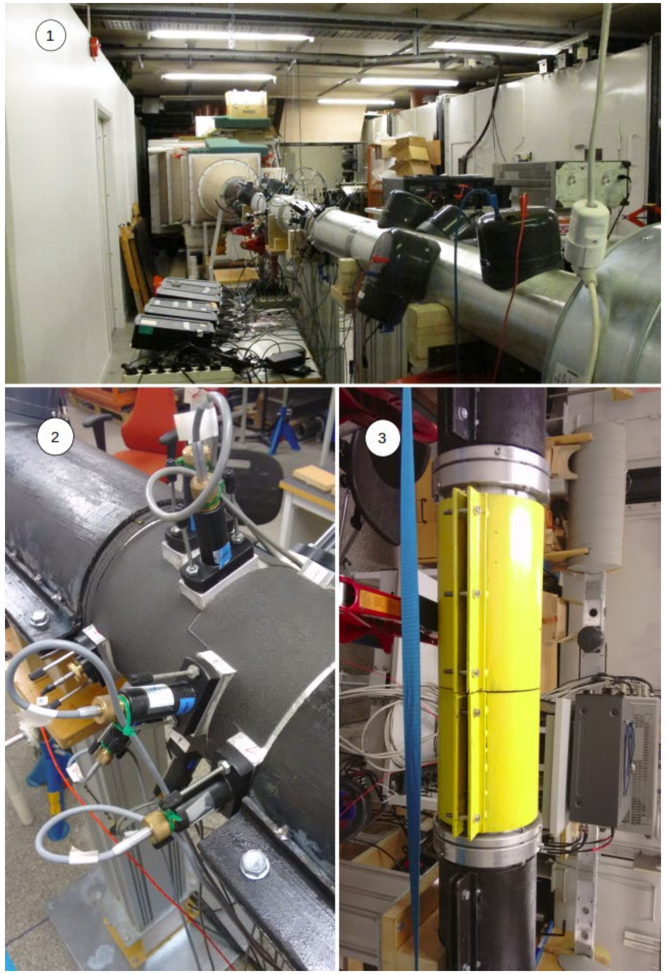

- **2x12 microphones** and **16 loudspeakers** in an optimised setup (max 6 modes)
- Aluminum pipe-sections with **constraint layer damping**
- Multi-channel excitation with algorithms for **simultaneous, uncorrelated excitation**
- **Modal decomposition** with **advanced** wave-numbers to account for damping
- Two stage measurements for **accurate scattering** and **source** characterisation

Orifice Measurements

Measurements for model-validation at the *Marcus Wallenberg Laboratory for Sound and Vibration Research at KTH*

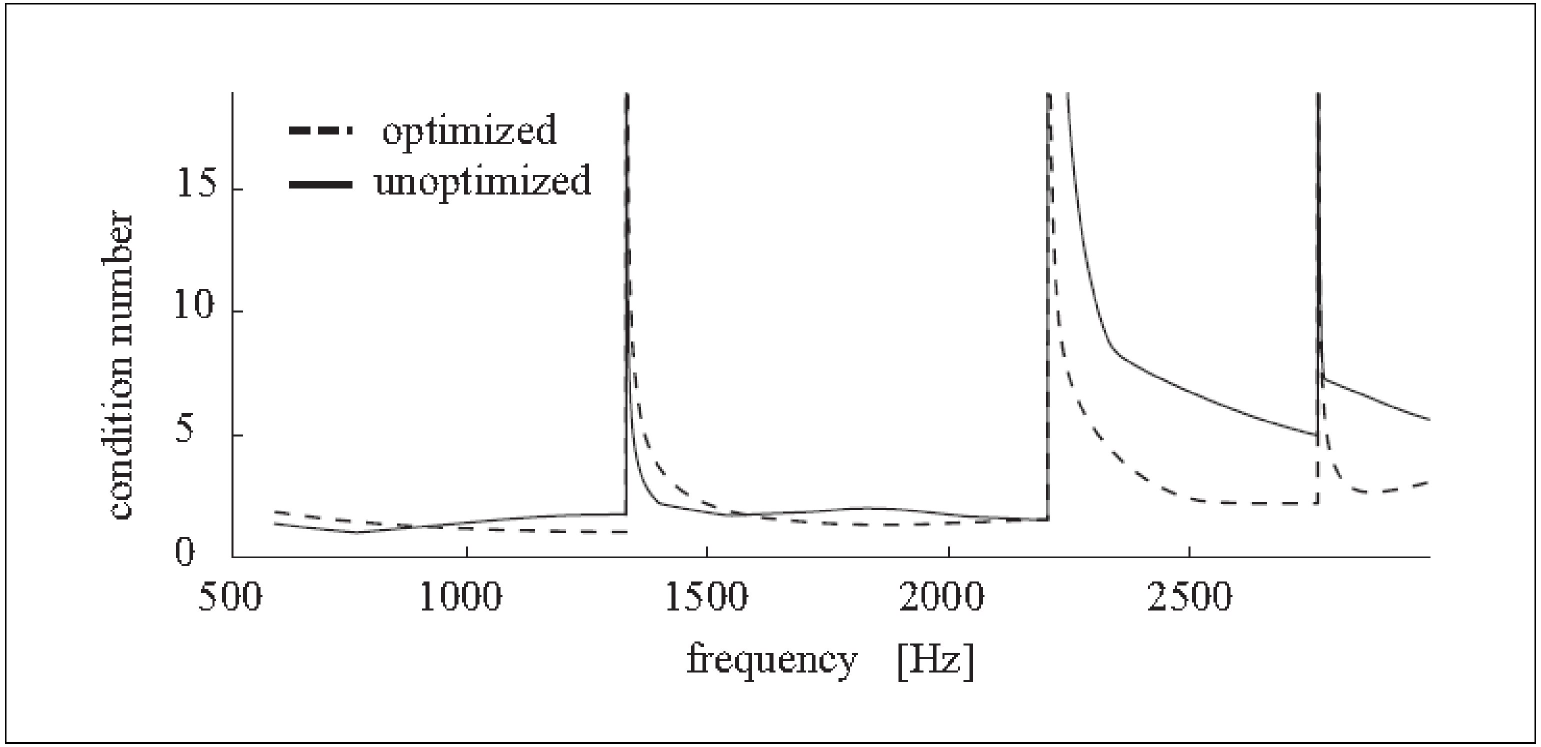

Figure from Ref. 12 showing the effect of optimizing the microphone configuration. Note the optimized configuration contains the minimum no. of mics for 6 modes (12) while the unoptimized contains 16 positions.

ers

t

for

n

n

Tandem Orifice - Scattering

Combining two multi-ports is a **multiplication** of their **transfer matrices**
Computing the **transfer matrix** is a **linear operation** on the scattering matrix

➡ **computational inexpensive**

2D distance

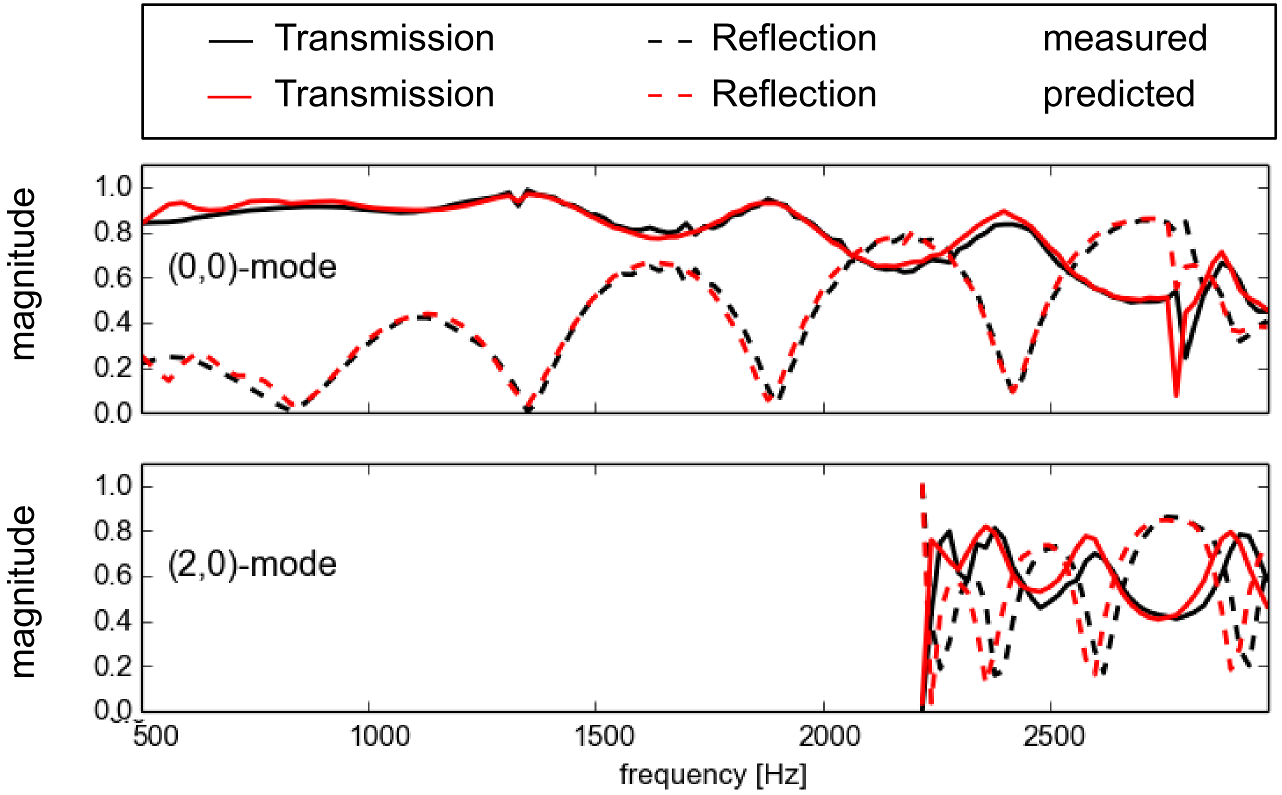

The scattering of an orifice plate is very little affected by disturbed inflow. Even for the shortest separation the Tandem case can be predicted using the Single orifice data.

Tandem Orifice - Source strength

For the source, the power **cross spectrum is computed**, **neglecting correlated sound sources** between the two multi-ports

➡ <u>This will cause aerodynamic installation effects when the flow fields</u> interact”

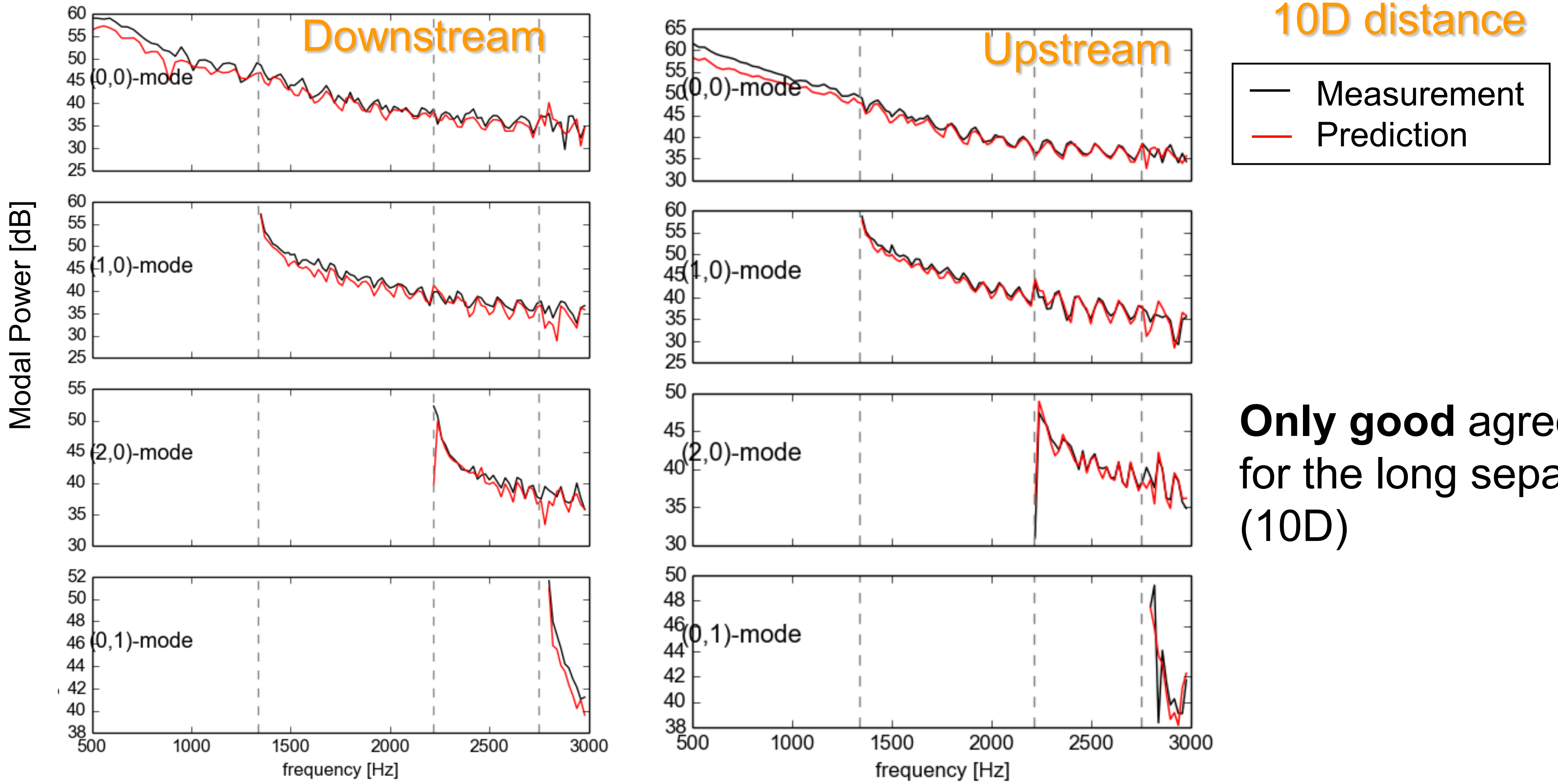

Only good agreement for the long separation (10D)

SUMMARY AND CONCLUSIONS

- The full multi-port approach gives a complete characterization of a duct element (scattering + sound generation)
- Applying the multi-port procedure to experimental or numerical data will eliminate the effect of boundaries i.e. represent the system under reflection free conditions
- The projection of pressure data on acoustic modes i.e. the basis of the modal decomposition used in the process will reduce the influence of hydro-dynamic disturbances (“turbulence”)
- Multi-port models have traditionally been applied to fluid machines, e.g., IC-engines and fans and the data (passive/active) determined experimentally

SUMMARY AND CONCLUSIONS

- The low frequency plane wave or 2-port case is today established in particular for the passive part
- In the IDEALVENT project the experimental procedures to determine multi-port data have been further developed
- In addition the usefulness of applying the same procedures on numerical data have been demonstrated for a number of cases

Reference list

1. Bodén, H. and Åbom, M., 1995. Modelling of fluid machines as sources of sound in duct and pipe systems. Acta Acustica 3, Dec., pp. 1-12.
2. J. Lavrentjev, M. Åbom and H. Bodén, 1995, A measurement method for determining the source data of acoustic two-port sources. *Journal of Sound and Vibration* 183, 517-531.
3. J. Lavrentjev and M. Åbom, 1995. A measurement method to determine the source-data of acoustic N-port sources. *Journal of Sound and Vibration* 197, 1-16.
4. M Karlsson, M Åbom (2010). Aeroacoustics of T-junctions –An experimental investigation. *Journal of Sound and Vibration* 329 (10), 1793-1808.
5. A. Holmberg, M. Åbom and H. Bodén (2011), “Accurate experimental two-port analysis of flow generated sound”. *Journal of Sound and Vibration*, DOI: 10.1016/j.jsv.2011.07.041.
6. H. Tiikoja, H. Rämmal, M. Åbom and H. Boden (2011). Investigations of Automotive Turbocharger Acoustics. *SAE Int. J. Engines* August 2011 4:2531-2542.
7. R. Kabral and M. Åbom (2018). Investigation of turbocharger compressor surge inception by means of an acoustic two-port model .Journal of Sound and Vibration, 412, 270-286. doi.org/10.1016/j.jsv.2017.10.003
8. Kierkegaard, A., Allam, S., Efraimsson, G and Åbom, M. (2012). Simulations of whistling and the whistling potentiality of an in-duct orifice with linear aeroacoustics. Journal of Sound and Vibration 331, 1084–1096.

Reference list

9. Alenius, E. (2012) *Flow Duct Acoustics: An LES Approach*. PhD thesis, KTH The Marcus Wallenberg Laboratory for Sound and Vibration Research, Stockholm, Sweden.
10. Alenius E., Åbom M. and Fuchs L., 2015. Large eddy simulations of acoustic-flow interaction at an orifice plate. *Journal of Sound and Vibration*, Vol. 345, pp 162-177.
11. Du L., Holmberg A., Karlsson M. and Åbom M., 2016. Sound amplification at a rectangular T-junction with merging mean flows. Journal of Sound and Vibration, Vol. 367, pp 69-83.
12. Sack, S., Åbom, M. and Efraimsson, G., 2016. On acoustic multi-port characterization including higher order modes. Acta Acoustica united with Acustica, ISSN 1610-1928, Vol. 192, nr 5, 834-850.
13. Shur, M., Strelets, M., Travin, A., Christophe, J., Kucukcoskun, K., Schram, C., Sack, S., Åbom, M., 2017. Experimental/Numerical Study of Ducted-Fan Noise: Effect of Duct Inlet Shape. AIAA Journal 56 (3), 979-996.
14. Sack, S., Åbom, M., 2017. Investigation of orifice aeroacoustics by means of multi-port methods. Journal of sound and vibration 407, 32-45.
15. Sack, S., Shur, M., Åbom, M, Strelets. M., Travin, A., 2017. Numerical eduction of active multi-port data for in-duct obstructions. Journal of Sound and Vibration 411, 328-345.